Novel Regulators of CXCL13 in Human CD4+ T Cells

This Thesis, Novel Regulators of CXCL13 in Human CD4+ T cells, presented by Isaac J Benque, and Submitted to the Faculty of The Harvard Medical School in Partial Fulfillment of the Requirements for the Degree of Master of Medical Sciences in Immunology has been read and approved by:

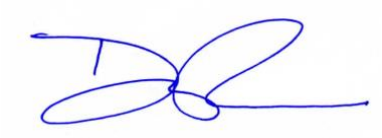

Dr. Deepak Rao, M.D. Ph.D

Dr. Vanessa Sue Wacleche, Ph.D

Date: 4/15/20

Novel Regulators of CXCL13 in human $CD4^+$ T cells

Isaac J. Benque

A thesis submitted to the Faculty of the Harvard Medical School

in Partial Fulfillment of the Requirement for the

Degree of Master's in Medical Sciences in Immunology.

Harvard University

Boston, MA

May 2020

Thesis Advisor: Deepak Rao, MD Ph.D. Isaac Benque

Novel Regulators of CXCL13 in human CD4$^+$ T cells

Abstract

Within chronically inflamed tissues, pathogenic T cell-B cell interactions can occur outside of secondary lymphoid organs to elicit the production of antibodies. The structure of these lymphoid aggregates depends on intercellular interactions and the production of crucial chemokines, including CXCL13. CXCL13 is essential in recruiting B cells to these aggregates as it binds CXCR5 on B cells and initiates chemotaxis. Patients with rheumatoid arthritis (RA) may develop T and B cell aggregates capable of generating antibodies locally. CXCL13 levels in RA synovium are associated with T-B cell aggregates, autoantibody production, and worsened disease. The source of CXCL13 in RA synovium is an expanded subset of T cells, termed T peripheral helper (Tph) cells. In human and primates, T follicular helper (Tfh) and Tph cells appear to be the dominant source of CXCL13; however, little is known about the extrinsic signals or the transcriptional regulators that induce T cells to produce CXCL13. In this project we have used CRISPR/Cas9 gene editing of primary human CD4$^+$ T cells to interrogate the roles of selected candidate regulators in altering CXCL13 production by human T cells.

Using this approach, deletion of BCL6, a critical transcriptional regulator of Tfh cells, inhibited the production of CXCL13 by human blood CD4$^+$ T cells from multiple donors. In additional, deletion of the aryl hydrocarbon receptor (AHR), a ligand gated transcription factor upregulated in Tph and Tfh cells, increased T cell production of CXCL13, demonstrating that AHR functions as a negative regulator of CXCL13 production. Deletion of the transcription factor POU2F1, a factor highly upregulated in both *ex vivo* and *in vitro* differentiated Tph cells, did not alter CXCL13 production, suggesting that POU2F1 is not an essential mediator of

CXCL13 production. Attempts to delete the additional candidates SOX4, a factor reported to regulate CXCL13 production, and RNF19A, an E3 ubiquitin ligase highly expressed in synovial tissue Tph cells, have not yet successfully altered target protein expression despite attempts with more than 5 guide RNAs for each target.

Together, the results present AHR as a new and robust negative regulator of CXCL13 and confirm BCL6 as a positive regulator of CXCL13 in $CD4^+$ T cells. Understanding how these regulators affect CXCL13 production in $CD4^+$ T cells may prove crucial in developing strategies to mitigate the formation of pathogenic T-B aggregates in autoimmune disease.

Table of Contents

List of Figures

Figure 5. CRISPR deletion of AHR in human $CD4^+$ T cells and the effect on CXCL13, IFNγ, IL-2, and IL-21 at day 4 and CXCL13 and IFNγ at day 11. (a) Flow cytometry histogram of AHR expression in $CD4^+$ T cells for 1 donor when CRISPR edited with control (blue) and AHR guides (red) (b) Western blot assessment of AHR deletion for 2 separate donors and quantification of band intensity normalized to B-Actin for control (CD8) and AHR deletion. Percent deletion of AHR as compared to control for 8 donors calculated using western blot band intensity. (c) CXCL13, IFNγ, IL-22, and IL-21 ELISAs 4 days after electroporation; 14 donors for CXCL13 and IFNγ, 4 donors for IL-22, 6 donors for IL-21. (d) CXCL13 and IFNγ ELISAs 11 days after electroporation; 8 donors for CXCL13 and IFNγ. IL-21 and IL-22 was not detected at day 11. Each symbol represents a donor and error bars are standard deviations. Unless otherwise indicated, differences are not significant. Statistics: ns, not significant ($P > 0.05$); * $0.01<P<0.05$; ** $0.001<P<0.01$; *** $0.0001<P<0.001$ (Wilcoxon signed rank test).

Figure 6. Deletion of POU2F1/OCT1 in human $CD4^+$ T cells and the effect on CXCL13 and IFNγ 4 days after electroporation. (a) Western blot analysis of POU2F1 deletion showing deletion using 2 guides in one donor. Percent deletion of POU2F1 as compared to control calculated using western blot band intensity; 4 donors for control, POU2F1 #2, and POU2F1 #3; 2 donors for POU2F1 #1 and POU2F1 #4. (b) CXCL13 and IFNγ ELISAs 4 days after electroporation; 4 donors for control, and POU2F1 #3; 6 donors for POU2F1 #2; 2 donors for POU2F1 #1 and POU2F1 #4. For the ELISAs, experimental conditions were normalized to control (CRISPR CD8) and the log base 2 of the standardized production of IFNγ and CXCL13 is plotted. Each symbol represents a donor and error bars are standard deviations. Unless otherwise indicated, differences are not significant.

Figure 7. Deletion of RNF19A in human $CD4^+$ T cells 4 days after electroporation. (a) Western blot analysis of RNF19A deletion using 7 guides in 2 donors per guide. Quantification of RNF19A band intensity normalized to B- Actin for control (CD8) and the 7 RNF19A guides. (b) Western blot analysis of RNF19A deletion using Synthego's multi-guide approach. Quantification of RNF19A band intensity normalized to B-Actin for control (CD8) and RNF19A with 2:1 sgRNA/Cas9 ratio, and RNF19A with 6:1 sgRNA/Cas9 ratio. (c) Insertion/Deletion (InDel) frequency based on DNA Sanger sequencing and calculated using TIDE (deskgen) for 3 guides; 2 donors for RNF19A #1 and RNF19A #3, 1 donor for RNF19A #2. (d) Real-Time quantitative PCR of cDNA from 2 donors 4 days post-electroporation and 2 donors 11 days post-electroporation with 4 RNF19A guides. Fold expression normalized to housekeeping gene RPL13A and calculated as $2^{-\Delta\Delta CT}$. Each symbol represents a donor and error bars are standard deviations. Unless otherwise indicated, differences are not significant.

Figure 8. Effect of RNF19A deletion in $CD4^+$ T cells on CXCL13 production 4 days and 11 days after electroporation. (a) Four days after electroporation, CXCL13 and IFNγ secretion for 4 donors in guide 1-4 and 2 donors in guides 9-11. (b) At day 4, CXCL13 and IFNγ secretion for 2 donors using Synthego's multi-guide approach against RNF19A and T cell Receptor Alpha-Chain (TRAC). Varying sgRNA/Cas9 tested: 2:1 sgRNA/Cas9 ratio and 6:1 sgRNA/Cas9 ratio. (c) CXCL13 and IFNγ secretion at day 11 from 4 donors using guides 1-4. For the ELISAs, experimental conditions were normalized to control (CRISPR CD8) and the log base 2 of the

standardized production of IFNγ and CXCL13 is plotted. Each symbol represents a donor and error bars are standard deviations. Unless otherwise indicated, differences are not significant.

List of Tables

Acknowledgments

I would like to thank Dr. Deepak Rao for providing me with excellent mentorship during my time in the lab. I greatly appreciated the guidance and support he provided on this project and my career in general. I would also like to thank Dr. Vanessa Wacleche, whose invaluable guidance was essential in completing this work and whose teaching instigated in me a scientific rigor in experimental designs. I also thank all of the Rao Lab for their continued help in this research project.

I would also like to thank Dr. Shiv Pillai for his mentorship and guidance in my education and career. I am very grateful for the continued support that Dr. Gavin Porter provides through his excellent teaching. I would also like to thank Dr. Michael Carroll, Selina Sarmiento, and the class of 2020 for making the MMSc in Immunology program a supportive and collaborative environment, especially Karishma Rupani, Kanupriya Kusumakar, Aarti Srivastava, Michelle Dong, and Diana Pena.

This work was conducted with support from Students in the Master of Medical Sciences in Immunology program of Harvard Medical School. The content is solely the responsibility of the authors and does not necessarily represent the official views of Harvard University and its affiliated academic health care centers.

Chapter 1: Background

1.1 T cell – B cell interactions

T cells and B cells interact with one another in order to induce a strong antibody mediated immune response[1]. These types of immune responses are generally thought to be mounted within secondary lymphoid organs (SLO) where T-B cell interactions are tightly and meticulously regulated through the help of chemokines and intercellular interactions[2]. However, within chronically inflamed tissues, T cells and B cells can form lymphoid aggregates capable of producing antibodies in the periphery[3]. A prime example of pathogenic T-B cell aggregate formation within inflamed tissue occurs in rheumatoid arthritis (RA).

1.2 Rheumatoid Arthritis

Rheumatoid arthritis (RA) is a systemic disease characterized by the inflammation of the synovium within the joints. If untreated, RA can lead to erosion and permanent damage to the joint. The disease may be influenced by the presence of varying risk factors and genetic predispositions[4]. In particular, certain variants of the D related (DR) locus within the human leukocyte antigen (HLA) class II loci have a strong association with RA[4]. Currently, most treatments seek to induce remission by broadly dampening inflammation, but there are no cures as of yet[4]. RA pathology is marked by high infiltrates of immune cells within the synovial sub-lining leading to joint damage.[4] These infiltrating cells include monocytes, B cells, $CD4^+$ T cells, and $CD8^+$ T cells[5]. Of these infiltrating immune cells, T and B cells may form aggregates in the synovium of seropositive RA patients ranging from small to large aggregate structures. About 15-20% of patients develop ectopic germinal centers whereby B cells can mature and produce antibodies[4,6,7]. Within the synovium, these B cells can produce anti-citrullinated peptide

antibodies (ACPA) or anti-IgG autoantibodies called rheumatoid factors (RF)[8,9]. Both autoantibodies have been associated with disease severity[10,11] and their levels correlate with the presence of T-B cell aggregates in the synovium[12]. Furthermore, the presence of aggregates correlates with more erosive and severe disease[6,13]. This indicates that understanding T-B cell interactions within the RA synovium may prove useful in mitigating disease severity and progression.

1.3 T Cells in the Context of RA

1.3.1 T Follicular Helper (Tfh) Cells

T cell - B cell interactions capable of eliciting a strong antibody response are generally thought to occur with secondary lymphoid organs (SLO). T follicular helper (Tfh) cells are the canonical B cell helper as they are recruited to SLOs where they orchestrate immune cell interactions by which B cells mature, differentiate, and produce specific antibodies. Tfh cells are marked by high expression of CXCR5 which binds CXCL13 and allows them to move to regions of high CXCL13 concentration, such as the B cell follicles[1]. Tfh cells also secrete large amounts of CXCL13 to attract $CXCR5^+$ B cells. Tfh cells then express a number of molecules necessary for B cell maturation and antibody production. For instance, CD40 ligand (CD40L) on Tfh cells interacts with CD40 on B cells to promote class-switching, and IL-21 secreted by Tfh cells can induce plasma cell differentiation and help B cells undergo Ig class switching and affinity maturation within germinal centers[14,15]. The master transcription factors that control the Tfh cellular program are BCL6 and MAF[1]. BCL6 is crucial in the differentiation and survival of Tfh cells while inhibiting alternative differentiation paths. BCL6 controls multiple aspects of the Tfh program, including promoting the expression of CXCR5, PD-1, ICOS, and CXCL13[16–18]. In RA,

an increased frequency of circulating CXCR5^{+} Tfh cells is noted[19]. These may participate in the generation of ACPAs and RF autoantibodies. RA synovium, however, contains very few CXCR5^{+} Tfh cells despite the presence of B cells and plasma cells[20].

1.3.2. T Peripheral Helper (Tph) Cells

Outside of secondary lymphoid organs, T cell and B cell interactions leading to antibody production can still occur. Notably, chronically inflamed tissues such as the synovium may contain T-B aggregates capable of producing antibodies[3]. In the synovium of seropositive patients, the lab recently reported that a subset of T helper cells was expanded. This subset of T cells, termed T peripheral helper cells (Tph) are characterized by high PD-1 expression, a lack of CXCR5, and the ability to induce plasma cell differentiation *in vitro*[20]. Tph cells (PD-1^{hi} CXCR5^{-} CD4^{+} T cells) secrete high levels of IL-21 and CXCL13. The production of IL-21 is controlled by the transcription factor MAF[18,21,22]. These cells are expanded in the circulation of systemic lupus erythematosus (SLE) patients, a disease characterized by breach of tolerance and the production of autoantibodies[21]. Tph cells have also been found to be involved in tumor immunity in breast cancer and lung cancer[23,24], in allograft rejection[25], and in autoimmune hepatitis[26]. We hypothesize that these cells may drive pathogenic aggregations of T and B cells in the periphery, leading to the production of harmful autoantibodies. Targeting these Tph cells may prove valuable in hampering disease progression while keeping homeostatic immunological functions intact.

1.3.3 Similarities and differences between Tfh and Tph Cells

Similarly to T follicular helper cells (Tfh), which help B cells mature within the follicle, Tph cells also have the ability to help B cells differentiate and produce antibodies[21]. Both cells express high levels of PD-1 and MAF, and both secrete high levels of CXCL13 and IL-21[3]. Although there are several similarities between Tfh and Tph cells, they differ in terms of their transcriptional and migratory programs. Tfh cells express BCL6 as its master transcription factor but Tph cells express low levels of BCL6 and upregulate its counter-regulator BLIMP1 instead[2]. Additionally, Tph cells do not express CXCR5 while Tfh cells do[3]. CXCR5 helps Tfh cells move down a CXCL13 concentration gradient so that they may interact with B cells at the T-B border within lymph node follicles. This, in turn, elicits a germinal center reaction, whereby antibodies are edited and refined through multiple rounds of selection to generate highly specific ones[2]. Contrary to Tfh cells, Tph cells express CCR2, CCR5, and CX3CR1, which allows them to move to inflamed tissue such as the synovium and help B cells mature there[20,21]. While some functions of Tfh and Tph cells overlap (production of CXCL13 and IL-21), their regulatory programs are distinct (Schematic 1). This indicates that uncharacterized regulators may play an essential role in controlling certain functions of these cells.

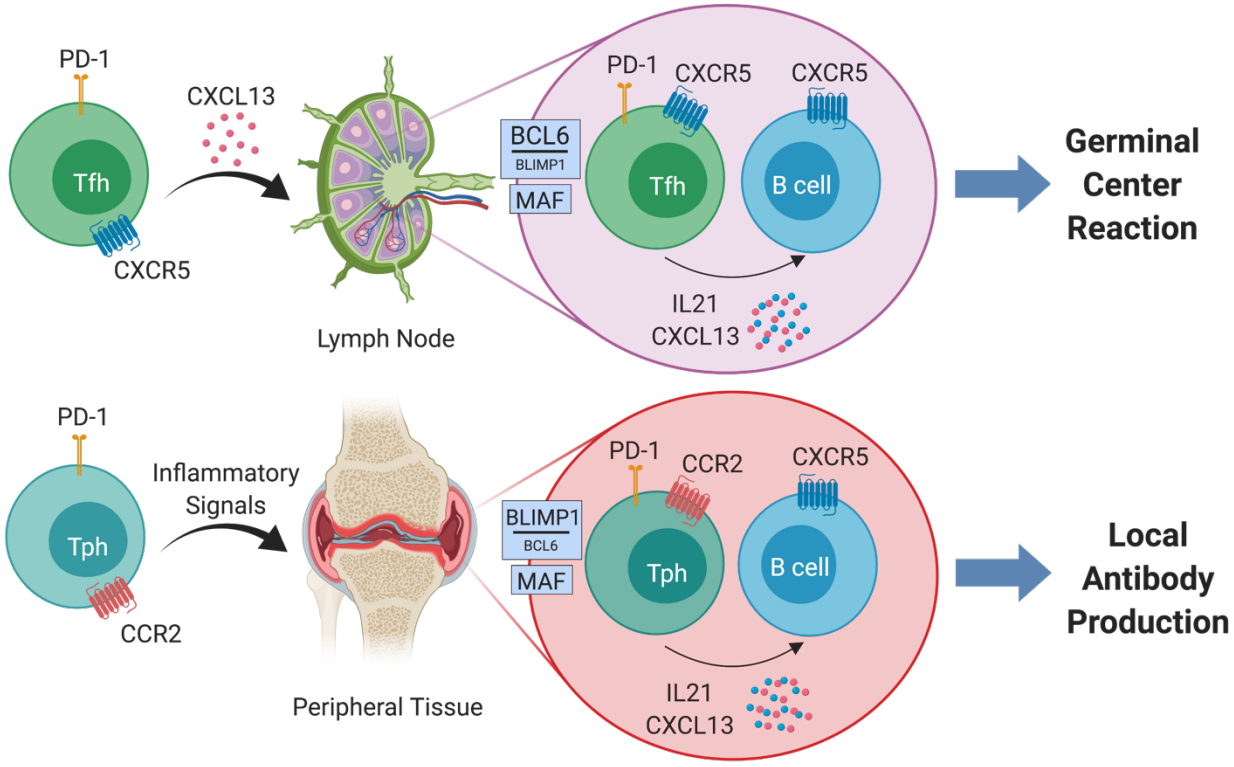

Schematic 1. Differences between Tph and Tfh cells. Adapted from Rao, D. A. *Frontiers in Immunology* (2018).

1.4 CXCL13

First called B Lymphocyte Chemoattractant (BLC), CXCL13 is a chemokine that binds CXCR5 and helps cells move to regions of high CXCL13 concentration through chemotaxis[27]. Within B cell follicles and germinal centers in lymph nodes, CXCL13 is essential in order to orchestrate the interactions between T and B cells[27]. The primary source of CXCL13 in the germinal center light zone is the follicular dendritic cells (FDCs)[28], but Tfh cells also produce high levels of CXCL13[1]. Both FDC and Tfh cells help recruit GC B cells to the light zone[1]. CXCL13 is also expressed in the germinal center of ectopic lymphoid follicles in the synovium of RA patients[29]. In RA, the levels of CXCL13 is associated with seropositivity status, severity

of the disease, and the presence of lymphoid aggregates[30]. CXCL13 may be necessary in establishing the formation of T-B cell aggregates and inducing the infiltration of B cells in tissues. Notably, the overexpression of CXCL13 downstream of an insulin promoter was sufficient to elicit the formation of tertiary lymphoid structures within pancreatic islets[31]. In RA, synovial samples with elevated CXCL13 contain more lymphoid aggregates and CXCL13 synovial and serum levels have been associated with more severe and erosive disease progression[33,34]. RNA-seq analysis indicates that the main source of CXCL13 in the synovium of RA patients are Tph cells, as opposed to monocytes, B cells, and fibroblasts[35].

In human secondary lymphoid organs, the two major sources of CXCL13 are Tfh cells and FDCs[1]. FDCs can arise in the context of tertiary lymphoid organs with germinal center follicles and can also secrete CXCL13[7,36]. However, FDCs are not apparent in T-B cells aggregates or diffuse immune cell infiltration of RA patients[7]. For RA patients with lymphoid neogenesis (aggregates that show characteristics of secondary lymphoid organs), FDCs are present in 15-28% of patient[36,37] but the presence of FDCs is only detected in later stages of lymphoid aggreggation[38]. Overall, FDCs are present in only 5-8% of RA patients[36,37]. Within these FDC^+ follicular aggregates, ACPA-producing plasma cells have been detected and these plasma cells express the enzyme activation-induced cytidine deaminase (AID), which is required for somatic hypermutations and class switching of antibodies[9]. Additionally, increase in the expression of AID correlates with the upregulated expression of CXCL13[9]. It is worth noting that CXCL13 is detected in the absence of FDCs in less organized aggregates[38], indicating that the production of CXCL13 may precede the appearance of FDCs within lymphoid aggregates. As opposed to FDCs, current evidence suggests that Tph cells serve as a major driver in the

aggregation of T cells and B cells outside of secondary lymphoid organs due to their high secretion of CXCL13 and presence prior to FDC^+ lymphoid aggregates.

1.5 Previously Reported Potential Regulators of CXCL13

The regulation of CXCL13 in $CD4^+$ T cells is not yet completely understood. Certain cytokines have been reported to be involved in CXCL13 production. For instance, TGF-β can induce the differentiation of CXCL13-producing $CD4^+$ T cells[39]. Activin A, which shares signaling cascade factors with TGF-β signaling such as Smad2-Smad3, can also promote CXCL13 production[40]. Contrary to TGF-β and Activin A, IL-2 inhibits CXCL13 production via STAT5[39]. The combination of TGF-B and neutralizing-IL-2 antibodies was best at inducing the differentiation of CXCL13-producing $CD4^+$ T cells as compared to TGB-β or anti-IL-2 antibodies alone[41].

In terms of transcription factors, the master transcription factor of Tfh, BCL6, was found to be involved in CXCL13 regulation as its overexpression in human $CD4^+$ T cells could enhance CXCL13 secretion 10-fold[18]. The transcription factor SOX4 is also reported to be involved in the generation of CXCL13-producing $CD4^+$ T cells downstream of TGF-β signaling[41]. SOX4 is part of group C of SRY-related HMG-box (SOX) family of transcription factors, which includes SOX11 and SOX12. Broadly, Sox4 regulates the development of T cells in the thymus of mice[42]. In peripheral T cells, Sox4 can also inhibit the differentiation of T cells into Th2 cells (T helper cell 2) by binding and negatively regulating Gata3, the master transcription factor of the Th2 program[43]. This effect was established to be downstream of TGF-β signaling via Smad2/3. The overexpression of Sox4 enhanced the secretion of IFNγ in Th1 polarization experiments. Although SOX4 is implicated in differentiating human naïve $CD4^+$ T

cells towards CXCL13-producing T cells[41], the role of SOX4 in differentiated $CD4^+$ T cells has not yet been established.

The incomplete knowledge of robust CXCL13 regulators in T cells may be due in part to the fact that mouse $CD4^+$ T cells do not produce CXCL13. CXCL13 production in the germinal centers comes primarily from FDCs in mice[1,28]. Therefore, studies of CXCL13 regulation in $CD4^+$ T cells need to be performed on human $CD4^+$ T cells.

1.6 Identification of New Candidate Regulators of CXCL13

Our lab aims to identify new CXCL13 regulators in $CD4^+$ T cells. By analyzing transcriptomic and CyTOF data sets, we selected a set of factors that associate with increased CXCL13 production.

1.6.1 Aryl hydrocarbon receptor (AHR)

CyTOF generated by the Accelerating Medicine Partnership (AMP) RA/SLE Network revealed that Tph cells are highly expanded in the circulation of lupus nephritis patients and RA patients[44]. From this data set, the expression of aryl hydrocarbon receptor (AHR) was elevated in both Tph and Tfh cells, suggesting a potential regulatory role for AHR in Tph and Tfh cellular programs. AHR is a ligand-activated transcription factor that detects environmental, dietary, microbial, and metabolic changes[45]. Upon binding of its ligand, cytoplasmic AHR translocates to the nucleus, where it can then control the transcription of various genes. AHR target genes contain an AHR binding DNA motif (5'-TNGCGTG-3') termed dioxin-responsive element (DRE)[46]. AHR can also associate with other transcription factors or lead to epigenetic changes by displacing histone deacetylase complexes and transcribing long non-coding RNAs which can

regulate the expression of other genes[47]. Apart from gene expression regulation, AHR is also known to have E3 ubiquitin ligase activity, leading to the proteasomal degradation of the estrogen receptor[48].

Within the immune system, AHR has multiple regulatory effects on adaptive immunity. Broadly, treatment with AHR agonists led to a decrease in cytotoxic T lymphocyte activity in mice[49] due to the induction of regulatory $CD4^+$ T cells by increasing the number of $Foxp3^+$ Treg cells[50]. Human naïve $CD4^+$ T Cells isolated from peripheral blood mononuclear cells (PBMCs) stimulated with plate-bound anti-CD3/CD28 and treated with IL-2 and AHR agonist TCDD led to the increased expression of FOXP3 and IL10 but did not change the expression of BCL6, BLIMP, or MAF[51]. This would indicate that AHR's effect in Tfh/Tph cells would be independent from inducing known regulators, but rather by being a novel regulator itself or inducing new regulators. Within type 1 regulatory T cells (Tr1 cells) capable of producing IL-10 without expressing FOXP3, AHR was shown to act in concert with cMAF to drive the expression of IL-10 in human[52] and to induce IL-21 in mice[53]. Notably, FOXP3 expression did not change when total human $CD4^+$ T cells were stimulated with PMA/ionomycin and treated with TCDD[54]. This would indicate that TCDD cannot act alone in pushing $CD4^+$ T cells towards a $FOXP3^+$ Treg. In humans and mice, AHR activation was also shown to contribute to the Th17 transcriptional program by increasing expression of IL-17 and IL-22[55,56]. Apart from these helper $CD4^+$ T cell subtypes, a role for AHR in the context of $CD4^+$ T cells that help B cells mature and produce antibodies has not yet been established.

Unpublished data from the Rao lab show that AHR is a potent negative regulator of CXCL13 by human $CD4^+$ T cells. Stimulation of human $CD4^+$ T cells in the presence of AHR agonist TCDD inhibits secretion of CXCL13, while treatment with AHR antagonist CH-22

increases CXCL13 production, in particular in the presence of TGF-β. Additionally, repeated stimulation dramatically increases the production of CXCL13 overtime and treatment with TCDD induces expression of the inhibitory receptor CD96. This work suggests that human T cells stimulated in the presence of TGF-β and with AHR suppressed differentiate into a CXCL13-producing phenotype with many features of Tph cells.

1.6.2. POU2AF1 & POU2F1

Unpublished RNA-sequencing data generated from sorted *ex vivo* Tph cells and *in vitro* differentiated CXCL13-producing T cell cells revealed that POU domain class-2-associating factor 1 (POU2AF1) is more highly expressed in *in vitro* and *ex vivo* Tph cells as compared to non-Tph cells. POU2AF1 (or BOB1, OCA-B) is a B cell transcriptional co-activator protein with no DNA-binding ability[57]. Instead, it associates with octamer motif-binding proteins OCT-1 (POU2F1) and OCT-2 (POU2F2), which can then bind DNA and influence transcription of target genes. In B cells, the POU2AF1-OCT1/2 complex regulates the expression of immunoglobulin genes. The expression of Pou2af1 is regulated by B cell receptor (BCR) signaling, CD40 ligand binding, and IL-4 signaling pathways[58]. It is also more highly expressed in mice germinal center B cells, further emphasizing its importance in producing antibodies.

As opposed to Pou2af1-deficient B cells, $CD4^+$ T cells deficient for Pou2af1 retained their ability to help B cells produce antibodies[58]. In the context of helper T cells, $Pou2af1^{-/-}$ mice show decreased levels of splenic and lymph node $CD4^+$ T cells as well as $CD8^+$ T cells and $B220^+$ B cells . $Pou2af1^{-/-}$ mice do not seem to control *Leishmania major* infections, which is mostly controlled by T cell helper 1 (Th1) immune responses. Pou2af1 appears to control the balance between Th1 and Th2 immune responses as $Pou2af1^{-/-}$ Th1 cells showed deficient IFNγ

whereas Pou2af1$^{-/-}$ Th2 cells produced more IL-4 and IL-13 than wild type (WT) Th2[59]. As opposed to changing the expression of Th1 master transcription factor T-bet, Pou2af1can bind the IFNγ promoter with the help of Oct-1 and Oct-2. Broadly, Pou2af1 and Oct-1 deficiencies can impair memory CD4^{+} T cell response as both are involved in regulating IL-2 secretion[60].

The role of POU2AF1 in Tfh cells is controversial. One group reported that POU2AF1 was more highly expressed in human Tfh cells, but Pou2af1-deficient Tfh cells in mice did not present with functional deficits as compared to WT Tfh cells[61]. The authors also found that the levels of Pou2af1 did not correlate with Cxcr5 and Bcl6. Another group noted the increased expression of Pou2af1 in Tfh cells and that Pou2af1$^{-/-}$ mice had decreased number of Tfh cells in secondary lymphoid organs[62]. Pou2af1$^{-/-}$ Tfh cells showed a decreased expression of Bcl6 as compared to WT Tfh cells. They showed that Pou2af1 bound to the *Bcl6* promoter with the help of Oct-1 and Oct-2 and induced its transcription. The role of POU2AF1 or OCT-1 has not yet been explored as a regulator of specific human Tfh functions, such as CXCL13 production, but OCT-1 is predicted to bind the promoter of CXCL13[63]. Since OCT-2 is more highly expressed in B cells, whereas OCT-1 is ubiquitously expressed[57], we chose to focus on the role of OCT-1 in T cells and whether it can influence CXCL13 production by CD4^{+} T cells.

1.6.3 RNF19A

Analysis of RNA-sequencing data from synovial immune cells revealed that the most differentially expressed gene between Tph cells and T cell subsets was CXCL13[5]. The second most differentiated gene was an RBR E3 ubiquitin ligase called Ring Finger Protein 19A (RNF19A) (data not shown). In RA, RNF19A is a memory CD4^{+} effector specific risk allele[64]. There are three main E3 ubiquitin ligases: the RING E3 ubiquitin ligases whose E2 conjugating

enzyme determines the ubiquitin chain type, the HECT E3 ubiquitin ligases whose C-terminus domain determines the identity of the ubiquitin chain, and RBR E3 ubiquitin ligases which determines the ubiquitination chain[65]. RNF19A is of the third kind and its E2 conjugating enzymes are UBE2L3 and UBE2L6. In ubiquitin chains, the ubiquitin moieties can be linked through one of their lysine residues (ex: K48, K63) or their N-terminal methionine residues (M1)[66]. The ubiquitin chains attached to proteins by E3/E2 ubiquitin ligases have varying roles depending on their linkage. For instance, RNF19A is known to ubiquitinylate TRAF6 in a K48 dependent manner to target TRAF6 to the proteasome for degradation[67]. TRAF6, on the other hand, can ubiquitinylate itself with the help of its E2 conjugating enzyme, UBC13 and UEV1A, in a K63-dependent manner to recruit factors important in NF-kB and AP-1 signaling[68]. RNF19A degradation of TRAF6 may influence T cell receptor (TCR) signaling as TRAF6 is involved in propagating signal downstream of CARD11-BCL10-MALT1 (CBM) complex; TRAF6 helps recruit the IKK complex responsible for phosphorylating the NF-kB inhibitor, IkBa[69]. Additionally, Traf6 was found to hinder IL-2 signaling as it bound Jak1 and negatively regulated the Jak1-Erk pathway in mice $CD4^+$ T cells[70]. This is of particular relevance as IL-2 hampered the generation of CXCL13-producing $CD4^+$ T cells[39,41]. Through proteasomal degradation of TRAF6, RNF19A may play a role in regulating IL-2 signaling. As of yet, however, the role of RNF19A in $CD4^+$ T cells has not been fully elucidated.

1.7 CRISPR of Primary Human Cells

In this project, we use CRISPR/Cas9 to determine the role of the aforementioned factors by deleting them and establishing the effects of their deletion. Recent advances in the CRISPR (Clustered, Regularly Interspaced, Short Palindromic Repeats) - Cas9 (CRISPR-associated

protein 9) system have allowed researchers to disrupt specific genes in primary cells with high efficiency[71]. Primary $CD4^+$ T cells are notoriously difficult to edit using CRISPR/Cas9 as the efficiency tends to be low, in particular because retroviral transduction does not yield stable Cas9 expression in primary human T cells[72]. Recent work by Marson and colleagues showed that electroporation of primary T cells with ribonucleoproteins (RNPs) leads to high efficiency deletion[73]. RNPs are a complex formed by the ligation of recombinant Cas9 protein to guide RNAs specific for a particular target. The guide RNAs consist of ligated trans-activating CRISPR RNA (trRNA) and CRISPR RNA (crRNA) or solely single guide RNAs (sgRNA). Once these RNP complexes are electroporated into the cells, the guide RNA recognizes its target genes and Cas9 creates a double stranded break (DSB). When the cell attempts to repair itself through non-homologous end joining (NHEJ), insertions and deletions can occur, resulting in the loss of protein expression or function[74]. A group at Genentech has recently optimized the use of RNP electroporation in primary T cell CRISPR editing resulting in >85% deletion efficiency[72]. As described in the following sections, we have adopted and further optimized this method in order to interrogate multiple candidate regulators of Tph cell function.

1.8 Goal and Hypothesis

Hypothesis:

Disrupting the production of CXCL13 in RA may hamper the formation of T and B cell aggregates within the synovium and understanding the regulation of CXCL13 may be essential in achieving that goal.

1. BCL6 deletion in $CD4^+$ T cells will not affect CXCL13 production as Tph express low amounts of BCL6 but still produce large amounts of CXCL13.

2. CRISPR deletion of SOX4 will decrease the production of CXCL13 as SOX4 was found to be involved in the differentiation of CXCL13-producing $CD4^+$ T cells.
3. Deletion of AHR from $CD4^+$ T cells will increase the production of CXCL13 as preliminary data suggest that pharmacologic treatment with AHR inhibitors increase CXCL13 production from $CD4^+$ T cells.
4. Deletion of OCT-1 and RNF19A will decrease CXCL13 production from $CD4^+$ T cells as preliminary data indicate that OCT-1 and RNF19A are more highly expressed in Tph cells.

Goal:

This project seeks to find strong regulators of CXCL13 in $CD4^+$ T cells by designing guide RNAs targeting genes of interest and establishing the effect of the deletion on CXCL13 production.

Chapter 2: Experimental Data

2.1 Introduction

In this chapter, I will discuss the strategy and approach used to determine the function of specific transcription factors in human $CD4^+$ T cells as they relate to CXCL13 production. The selected factors include BCL6, SOX4, AHR, POU2F1, and RNF19A. Using CRISPR/Cas9, we established the effect of their deletion from primary $CD4^+$ T cells on CXCL13 production.

2.2 Materials and Methods

2.2.1 Human PBMC processing: Blood samples were collected in leukoreduction collars obtained from healthy donors at Brigham and Women's Hospital. PBMC were isolated by density centrifugation using Ficoll-Paque PLUS density gradient media (General Electric) in 50 mL Falcon tubes. PBMCs were cryopreserved in FBS (Gibco) with 10% DMSO at -180°C following isolation.

2.2.2 T cell Isolation: PBMCs were thawed in RPMI with 10% FBS and rinsed twice. PBMCs were then counted. PBMCs were washed in MACS buffer once. Memory $CD4^+$ T cells were isolated from PBMCs through negative selection using Human Memory $CD4^+$ Isolation Kit (Miltenyi Biotec). For antibody staining, 10 uL of MACS buffer per 10^7 PBMCs and 10 uL of Memory $CD4^+$ T cells antibody cocktail per 10^7 PBMCs was added and incubated for 10 minutes at 4°C. For microbeads ligation, 20 uL of MACS buffer per 10^7 PBMCs and 20 uL of anti-biotin microbeads per 10^7 PBMCs was added and incubated for 15 minutes at 4°C. The cells were washed in MACS buffer once and memory $CD4^+$ T cells were eluted from LS columns (Miltenyi Biotec) placed in a magnetic field. Human $CD4^+$ T cells were isolated and cultured at 1 million per well on a 48-well plate in complete media (RPMI with 10% FBS, 1% Pen/Strep, 1%

Glutamine, 1% Hepes) and stimulated for 2 overnights with anti-CD3/CD28 dynabeads (1:5 beads/cells ratio).

2.2.3 Guide RNA design: The guides were designed to preferentially target early exons and have high on-target efficiency and low off-target effects. The guides were designed using DeskGen, CHOPCHOP, the Broad Institute's sgRNA Designer: CRISPRko, IDT, and Synthego. The guide sequences, type of guides, and design programs are described in Table 1. All guides were purchased from Integrated DNA Technology (IDT).

2.2.4 CRISPR electroporation: RNP complexes were assembled by incubating the guide RNA (gRNA) and transactivating crRNA (trRNA) (1:1 trRNA/gRNA ratio) for 2 minutes at 95°C. The individual guide RNAs and sgRNA used were ordered from IDT and can be found in Table 1. Guide RNAs targeting CD8 were used as a negative control. After cooling, spCas9 (Macrolab) was added (1:2 Cas9/gRNA-trRNA ratio, unless otherwise indicated) and incubated at 37°C for 1 hour. When using the Synthego kit, all three sgRNA against RNF19A were pooled together and the ratio of Cas9 to sgRNA varied as indicated.

The cultured memory $CD4^+$ T cells (see section 2.2.2) were harvested and washed with PBS and the dynabeads were removed with a magnet. The cells were electroporated with the RNP complexes with the 4D nucleofector (Lonza) using the EH-115 pulse and P3 Primary 4D X Kit (Lonza). Where indicated, RNP complexes were incubated with the 2B nucleofector according to the T23 pulse and using Amaxa Human T cell Nucleofector Kit (Lonza). Electroporated cells were incubated in complete media with 2 ng/mL TGF-β and anti-CD3/CD28 dynabeads (1:5 beads/cells ratio) for 4 days. At day 4, some experiments cells were reset, washed in PBS, and dynabeads were removed with a magnet. The cells were then incubated again for 7

days in complete media with 2 ng/mL TGF-β and anti-CD3/CD28 dynabeads (1:5 beads/cells ratio). When indicated, at day 4 and day 11, the cells were collected and aliquoted for flow cytometry or western blotting, and DNA sequencing. The supernatant was also collected at both time points for ELISAs.

2.2.5 Western Blotting: Cells were lysed in Rip A lysis buffer (150 mM NaCl, 1% Nonidet P-40 (Sigma-Aldrich), 0.5% Sodium deoxycholate, 0.1% SDS, Complete Protease Inhibitor cocktail (Roche), 50 mM Tris HCl) for 90 minutes on ice. Samples were centrifuged and supernatant was transferred and stored at -80°C in new eppendorf tubes. The protein concentration was calculated using BCA protein assay kit (Pierce) according to the manufacturer's protocol. Samples were run on 12-well 10% Criterion TGX Precast Gels (Bio-Rad) for 2 hours at 120 Volts. About 2-15 μg of protein was loaded per lane. The protein was transferred to 0.2μm PVDF membrane (Bio-Rad) using the Bio-Rad Trans-Blot Turbo Transfer System. The membrane was blocked in Tris-buffered saline with 0.1% Tween 20 (TBST) and 5% milk (Cell Signaling). The membrane was incubated overnight at 4°C with primary antibodies diluted in 5% milk TBST. Primary antibodies used are as follows: 1:1000 rabbit anti-AHR (D5S6H, Cell Signaling), 1:10000 anti-β-Actin (BA3R, Invitrogen), 1:500 anti-SOX4 (AB5803, SigmaAldrich), 1:200 anti-SOX4 (B7, Santa Cruz), 1:500 anti-SOX4 (ab80261, abcam), 1:400 anti-RNF19A (NBP1-87989, Novus), 1:500 anti-RNF19A (PA5-54861, Invitrogen), 1:1000 anti-OCT1 (A301-717A, Bethyl). After washing in TBST, the membrane was incubated with HRP-conjugated secondary antibodies diluted in TBST for 1 hour. Secondary antibodies used are as follows: 1:10000 anti-Mouse IgG-HRP conjugated (115-035-146, Jackson), 1:5000 anti-Mouse IgG-HRP conjugated (sc-516102, Santa Cruz), 1:5000 anti-Rabbit IgG-HRP conjugated (711-035-152, Jackson). After washing in TBST, the membrane was incubated with Clarity Western ECL Substrate (Bio-Rad) for 5

minutes and 2 minutes when staining for Actin. The membrane was exposed using Bio-Rad Chemidoc and chemiluminescent and colorimetric exposures were recorded. Images were analyzed using Image Lab (Bio-Rad). For further detection of other proteins, the membrane was stripped using Restore Western Blot Stripping Buffer (Thermo Scientific) for 15 minutes at 37°C. HRP was deactivated by incubating the membrane with TBST with 1% Sodium Azide for 15 minutes at room temperature. After washing, the membrane was blocked and blotted again as previously described.

2.2.6 Flow Cytometry: Memory $CD4^+$ T cells were washed once in PBS and stained with Live/Dead Fixable Aqua cell stain (Invitrogen, L34957) for 15 minutes at 23°C. After washing in PBS/1% BSA, the cells were stained with cell surface marker antibodies for 15-30 minutes at 4°C. For intracellular staining, the cells were fixed and permeabilized using Transcription Factor Staining Buffer Set (Invitrogen). The cells were then stained with the intracellular markers for 30 minutes at 4°C and where applicable, 60 minutes at room temperature for intranuclear staining. After washing with permeabilization buffer and PBS/1% BSA, the cells were run on a BD LSRFortessa. The data were analyzed using FlowJo 10.4.

Antibodies were purchased from BioLegend unless indicated otherwise. In the CRISPR deletion of PD-1 the antibodies used were: anti-CD4-FITC (clone: RPA-T4) or anti-CD4-Alexa700 (clone: RPA-T4), anti-CD3-PE-Cy7 (clone: HIT3a), anti-PD-1-APC (clone: EH12.2H7), anti-CD8-BV711 (clone: RPA-T8), and Live/dead fixable Aqua Dead Cell Stain kit (Invitrogen). In the CRISPR deletion of MAF and AHR the antibodies used were: anti-CD4-Alexa700 (clone: RPA-T4), anti-CD3-PE-Cy7 (clone: HIT3a), anti-PD-1-APC (clone: EH12.2H7), anti-CD8-BV711 (clone: RPA-T8), anti-MAF-BV421 (clone: symOF1), anti-AHR-PE (clone: FF3399), and Live/dead fixable Aqua Dead Cell Stain kit (Invitrogen). In the CRISPR

deletion of BCL6 the antibodies used were: anti-BCL6-APC (eBioscience, clone: Bcl-up) anti-CD8-BV711 (clone: RPA-T8), anti-CD3-AF700 (clone: 17A2), anti-CD4-BUV395 (BD Bioscience, clone: RPA-T4), anti-AHR-PE (clone: FF3399), anti-PD-1-PE/Cy7 (clone: EH12.2H7), and Live/dead fixable Aqua Dead Cell Stain kit (Invitrogen).

2.2.7 Detection and Quantification of Cytokines: Concentrations of cytokines in supernatants from CRISPRed cells were measured through ELISA using the following kits according to their protocol: Human CXCL13/BLC/BCA-1 DuoSet ELISA (R&D, cat#: DY801), Human IFN-gamma DuoSet ELISA (R&D, cat#: DY285B), IL-21 Human Uncoated ELISA kit (Invitrogen, cat#: 88-8218-88), Human IL-2 DuoSet ELISA (R&D, cat#: DY202). HRP activated using TMB Substrate Kit (ThermoFisher).

2.2.8 DNA isolation and sequencing: DNA was isolated from cells using DNeasy Blood & Tissue Kit (Qiagen) according to the manufacturer's protocol. Polymerase chain reaction (PCR) using Q5 High-Fidelity PCR Kit (New England BioLabs) was perfomed on the T100 Thermal Cycler (Biorad). The primers used were as follows: *RNF19A #1* (forward: 5'- ACTGGAACCA-TGACTACAAGAAGTT-3'; reverse: 5'-TCCACATAGAAACCCTTCCCC-3'), *RNF19A #2* (forward: 5'- TGAACTCAGAATTTAAAGGGGAAAA-3'; reverse: 5'- TCAGAACATTTTA-AAGCAAGTCTGC-3'), *RNF19A #4* (forward: 5'- AACACTGACCCTGTCTCAATTCT-3'; reverse: 5'- ATCATGGGGATTAAACCGTTCAG-3'). PCR products were sent to Eurofin for Sanger sequencing. Efficiency of CRISPR was assessed by the percent insertions/deletions induced as compared to control with TIDE (Tracking of Indels by Decomposition, Deskgen).

2.2.9 Quantitative Real Time PCR (RT-PCR): RNA from cells was isolated using the RNeasy Mini Kit (Qiagen) according to their protocol. cDNA was generated from RNA using the

Quantitect Reverse Transcription kit (Qiagen). RT-PCR of the cDNA was run with Brilliant III SYBRGreen (Agilent Technologies) on the AriaMX Real-Time PCR System. Primers used were as follows: *RNF19A* (forward: 5'-TGTGGCAACTGGGAACACTG-3'; reverse: 5'-TCCACTTGCACTCAAACTGC-3'), *RPL13A* (forward: 5'-CATAGGAAGCTG-GGAGCAAG-3'; reverse: 5'-GCCCTCCAATCAGTCTTCTG-3'). All primers were purchased from Integrated DNA Technologies (IDT). PCR product has an approximate size of 473 base pairs. Expression levels relative to housekeeping gene RPL13A were calculated according to the $2^{-\Delta\Delta Ct}$ formula.

2.2.10 Statistical testing: Data are presented as mean ± standard deviation (SD). To assess statistical significance, two-sided Student's t tests and Wilcoxon signed rank test were used where indicated. Statistics: ns, not significant ($P > 0.05$); * $0.01<P<0.05$; ** $0.001<P<0.01$; *** $0.0001<P<0.001$; **** $P < 0.0001$. PRISM was used for all statistical testing.

2.3 Results

2.3.1 Primary human CD4$^+$ T cells can be edited using RNP electroporation at high efficiency

We first started by testing the efficiency of the assay by CRISPR deleting PD-1 from human primary CD4$^+$ T cells through electroporating RNP complexes into cells using two different instruments: Lonza's 2B nucleofector and 4D nucleofector. The 2B nucleofector is a single cuvette system with an electroporation volume of 100 uL whereas the 4D nucleofector is a multi-cuvette strip system containing 16 wells with an electroporation volume of 20 uL each. As compared to the 2B nucleofector, the 4D nucleofector allows for faster electroporation of all experimental conditions within one experiment. The efficiency of PD-1 deletion was established by comparing deletion of PD-1 to a negative control gRNA targeting CD8, which should not affect CD4$^+$ T cells. Electroporation using the Lonza 4D nucleofector yielded a CRISPR deletion efficiency above 90% in 4 donors as measured by the surface expression of PD-1 through flow cytometry **(Fig 1a, 1b)**. The Lonza 2B nucleofector had a substantially lower efficiency as from 2 donors, the highest efficiency was 65% **(Fig 1b)**. We therefore chose to use the 4D nucleofector in subsequent experiments.

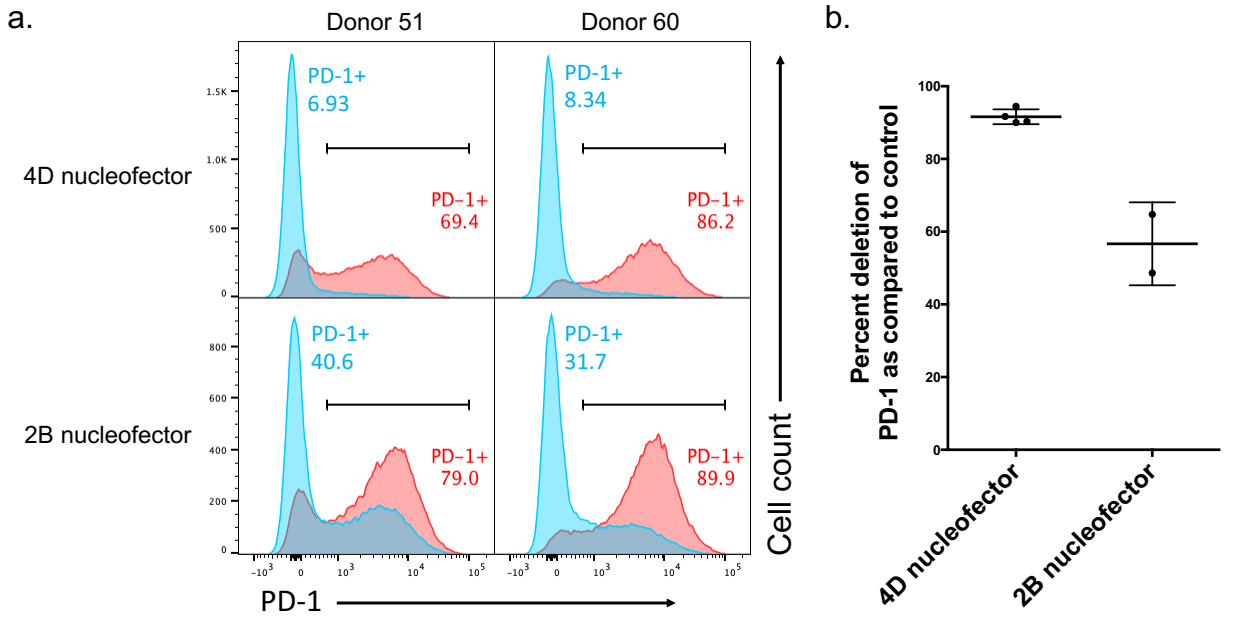

Figure 1. PD-1 deletion in primary human $CD4^+$ T cells 4 days after electroporation using the 4D nucleofector and 2B nucleofector. (a) Flow cytometry histogram plots of PD-1 expression in $CD4^+$ T cells of 2 donors 4 days after electroporation using the 2B nucleofector and 4D nucleofector. Blue: PD-1 CRISPR; Red: Control (CD8) CRISPR. Gated on lymphocytes, single cells, live cells, and $CD4^+CD3^+$ cells. (b) Quantification of flow cytometry data: percent deletion of PD-1 from 4 donors using the 4D nucleofector and 2 donors using the 2B nucleofector. Each symbol represents a donor and error bars are standard deviations. Statistics: ns, not significant ($P > 0.05$); ** $0.001<P<0.01$ (two-tailed Student's t-test).

To test the efficiency of the assay on a transcription factor, we knocked out MAF from $CD4^+$ T cells. Four days after electroporation, the expression of MAF was decreased when MAF was CRISPRed compared to negative control (CRISPR CD8) as measured through flow cytometry (**Fig 2a**). This deletion of MAF reduced the production of IL-21 from $CD4^+$ T cells by approximately half in 2 independent donors. These results confirms recent observations published by our group[21]. In contrast, the production of CXCL13 was not affected by the deletion of MAF **(Fig 2b)**.

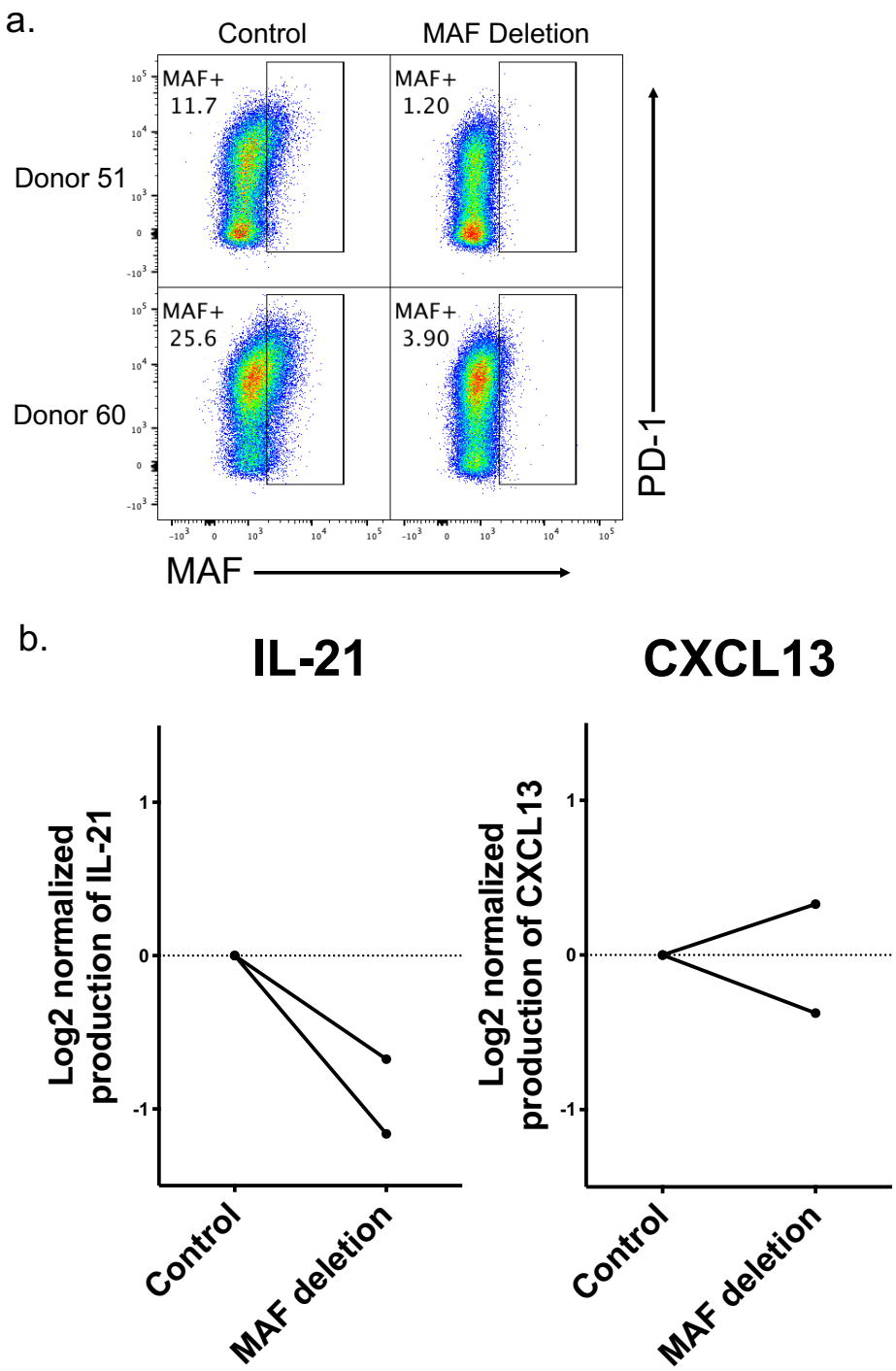

Figure 2. CRISPR deletion of MAF in human CD4$^+$ T cells and the effect on CXCL13 and IL-21 secretion 4 days after electroporation. (a) Flow cytometry plot of PD-1 vs. MAF expression at day 4 for 2 donors on CD4$^+$ T cells (b) Production of IL-21 and CXCL13 as measured by ELISA in 2 donors. For the ELISA, experimental conditions were normalized to control (CRISPR CD8) and the log base 2 of the standardized production of IL-21 and CXCL13 is plotted. Each symbol represents a different donor.

2.3.2 Interrogation of candidate regulators of CXCL13 production by CRISPR

Here we present results of studies aimed at evaluating the effects of five potential regulators of CXCL13 production in human $CD4^+$ T cells: BCL6, SOX4, AHR, POU2F1, and RNF19A. We present progress made in attempt to delete each of these factors and, if successful, establish the effect of its deletion on CXCL13 production.

2.3.2.1 <u>BCL6</u>

BCL6 is critical transcription for Tfh cells, and lentiviral overexpression of BCL6 in human $CD4^+$ T cells has been reported to increase CXCL13 production[18]. We tested 4 guides targeting BCL6, and all decreased the frequency of BCL6+ cells. As measured by flow cytometry, guide BCL6 #1 decreased the frequency of BCL6+ cells by a factor of 2, guide BCL6 #2 decreased the frequency of BCL6+ cells by 1.3 fold, BCL6 #3 decreased the frequency of BCL6+ cells by 1.8 fold, and BCL6 #4 decreased the frequency of BCL6+ cells by 2.6 fold **(Fig 3a)**. We conclude therefore that guide #4 is the most efficient at knocking out BCL6 from $CD4^+$ T cells. When guide #4 was tested in 6 donors, the production of CXCL13 was reduced on average by 2.2 fold as compared to control (CD8) but the production of IFNγ was not altered **(Fig 3b)**. IFNγ serves as a control to assess whether production of a distinctly regulated cytokine is unaffected. Guides #1 and #3 showed a slight decrease in CXCL13 production in $CD4^+$ T cells from 2 donors while having no discernable effect IFNγ **(Fig 3b)**. The use of guide #2 did not seem to alter CXCL13 or IFNγ production in 2 separate donors. These data indicate a positive regulatory role for BCL6 in the production of CXCL13 from human $CD4^+$ T cells.

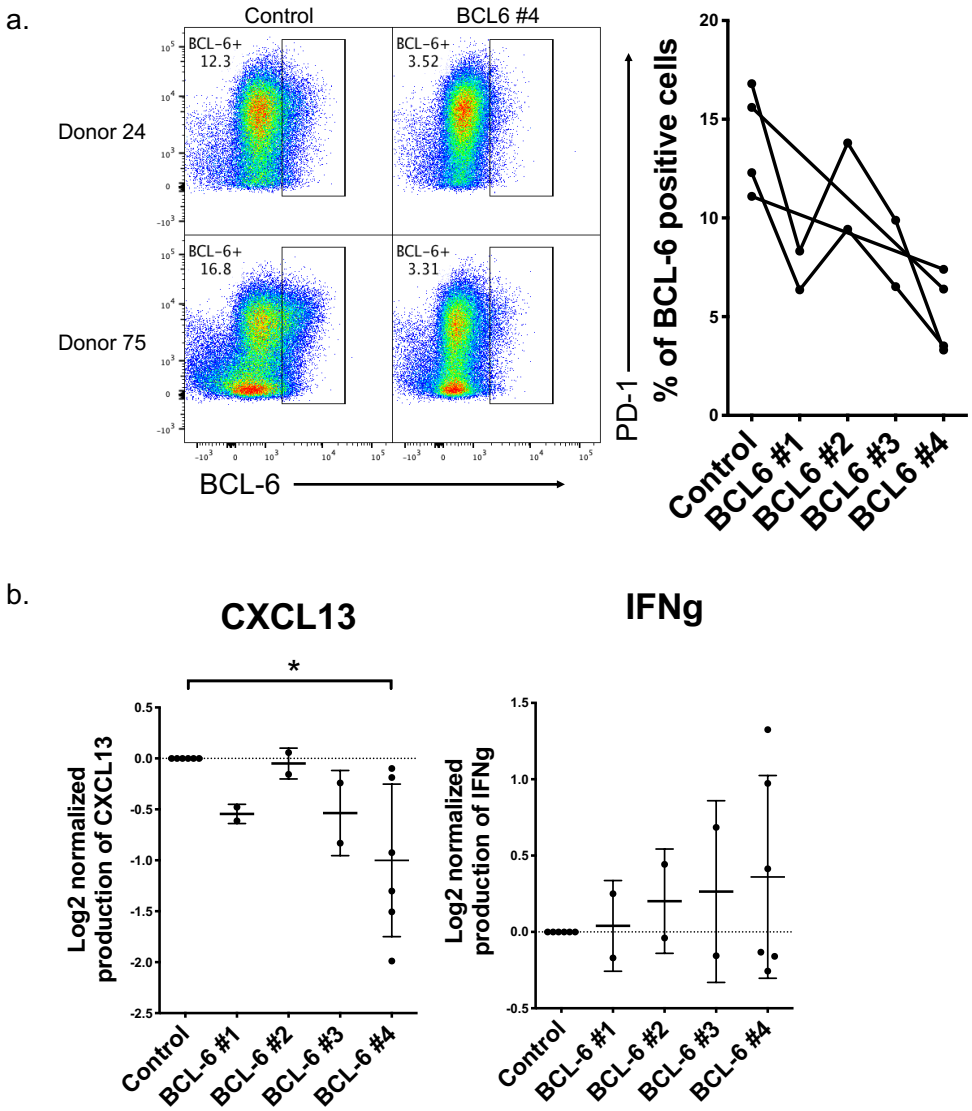

Figure 3. CRISPR deletion of BCL6 in human CD4$^+$ T cells and the effect on CXCL13 and IFNγ 4 days after electroporation (CRISPR performed in collaboration with Dr. Wacleche). (a) Flow cytometry plot of PD-1 vs. BCL6 expression in CD4$^+$ T cells at day 4 using control (CD8) and guide BCL6 #4 in 2 donors. Quantification of flow cytometry data: percent of BCL6 positive cells using 4 CRISPR guides against BCL6 in 2 separate donors, except guide #4 which was tested in 4 donors. (b) CXCL13 and IFNγ secretion measured 4 days after electroporation. There are 2 donors per guides except for guide #4 which has 6 donors. For the ELISAs, experimental conditions were normalized to control (CRISPR CD8) and the log base 2 of the standardized production of IFNγ and CXCL13 is plotted. Each symbol represents a donor and error bars are standard deviations. Unless otherwise indicated, differences are not significant. Statistics: ns, not significant ($P > 0.05$); * $0.01 < P < 0.05$ (Wilcoxon signed rank test).

2.3.2.2 SOX4

Overexpression of SOX4 in naïve $CD4^+$ T cells has been reported to increase CXCL13 production[41]. We attempted to CRISPR delete SOX4 in $CD4^+$ T cells using a multitude of guide RNAs and single guide RNAs. Western blots of whole $CD4^+$ T cell lysates did not show altered SOX4 expression in the first 4 guides used **(Fig 4a, 4b)**. Instead of guide RNAs that need to be ligated to trRNAs prior to RNP formation, we then tested the use of different single guide RNAs (SOX4 #5 & 7) which can directly bind to Cas9. Again the expression of SOX4 remained unaltered with the single guides **(Fig 4a, 4b)**. To confirm that the band evaluated by western blot is indeed SOX4, we also tested different SOX4 primary antibodies. Across all 3 antibodies tested, the expression of SOX4 remained strong in the experimental conditions. All 6 guides against SOX4 used did not alter the secretion of CXCL13 4 days post-electroporation except for guide SOX4 #7 **(Fig 4c)**. As expected, none of the guides altered IFNγ production at day 4 **(Fig 4c)**. Eleven days after electroporation, the first 4 guides tested did not alter CXCL13 or IFNγ secretion from $CD4^+$ T cells **(Fig 4d)**. Therefore, the role of SOX4 remains unclear as additional work is required to robustly alter SOX4 expression.

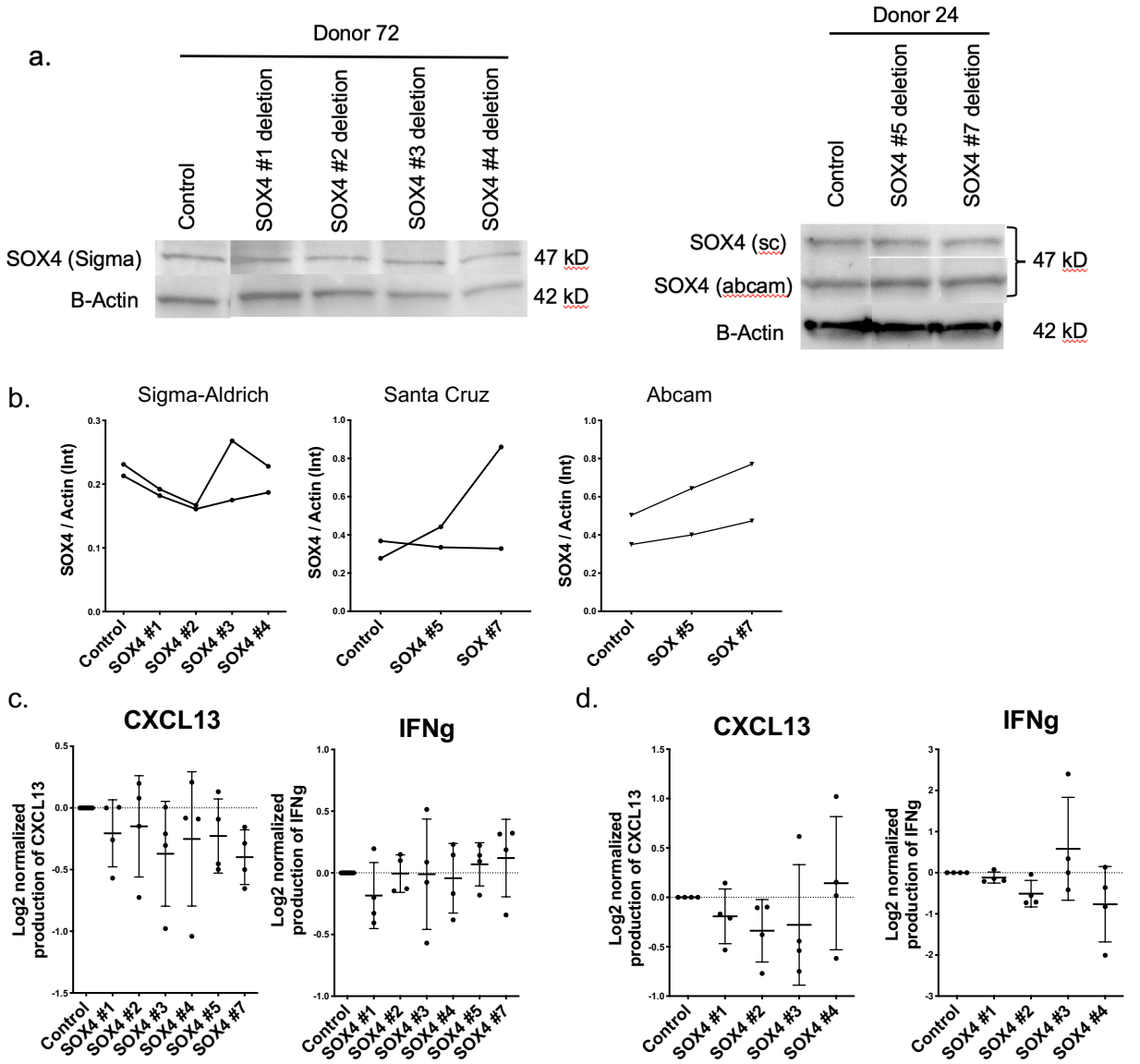

Figure 4. CRISPR deletion of SOX4 in human CD4$^+$ T cells and the effect on CXCL13 and IFNγ secretions 4 and 11 days after electroporation. (a) Western blot of whole CD4$^+$ T cells lysates of 2 donors 4 days after electroporation. 6 guides were tested and 3 anti-SOX4 antibodies were used. (b) Quantification of band intensity for the three antibodies and the 6 guides used. Each symbol is a separate donor. The band intensities were normalized to the B-Actin. CXCL13 and IFNγ secretion measured 4 days (c) and 11 days (d) after electroporation. There are 4 donors per guide; 6 guides for day 4; 4 guides for day 11. For ELISAs, experimental conditions were normalized to control (CRISPR CD8) and the log base 2 of the standardized production of IFNγ and CXCL13 is plotted. Each symbol represents a donor and error bars are standard deviations.

2.3.2.3 AHR

Preliminary analysis of CyTOF data indicate that AHR is more highly expressed in Tph and Tfh cells (data not shown). Additionally, unpublished work from the Rao lab has shown that treatment of $CD4^+$ T cells with AHR agonists decreases production of CXCL13 while treatment with AHR antagonist increases CXCL13 production (data not shown). Here, CRISPR deletion of AHR was successful as assessed by flow cytometry and confirmed through western blotting **(Fig 5a, b).** Because detection of AHR by flow cytometry can be ambiguous, we used western blotting to establish the efficiency of the deletion. AHR deletion was highly efficient as its percent efficiency averaged at 87% for 8 donors **(Fig 5a)**. Four days after electroporation, AHR deletion in human $CD4^+$ T cells increased the secretion of CXCL13 by 3.11 times (**Fig 5c)**. The deletion of AHR increased the secretion of IFNγ at day 4. As AHR is known to regulate IL-22 secretion positively, we measured IL-22 production and found that AHR deletion decreased IL-22 levels by 1.5 fold on average. In order to assess other B cell helper functions of $CD4^+$ T cells, we measured IL-21 and found that AHR deletion did not alter the production of IL-21. Eleven days after electroporation, CXCL13 secretion was 10-fold higher than at 4 days post-electroporation in the control **(Fig 5c, d)**. The deletion of AHR maintained increased production of CXCL13 from $CD4^+$ T cells at day 11, but there was no effect on IFNγ production between control (CD8) and AHR deletion **(Fig 5d)**. The levels of IL-22 and IL-21 were undetectable 11 days after electroporation. This data suggest that AHR is a novel regulator of CXCL13 in human $CD4^+$ T cells.

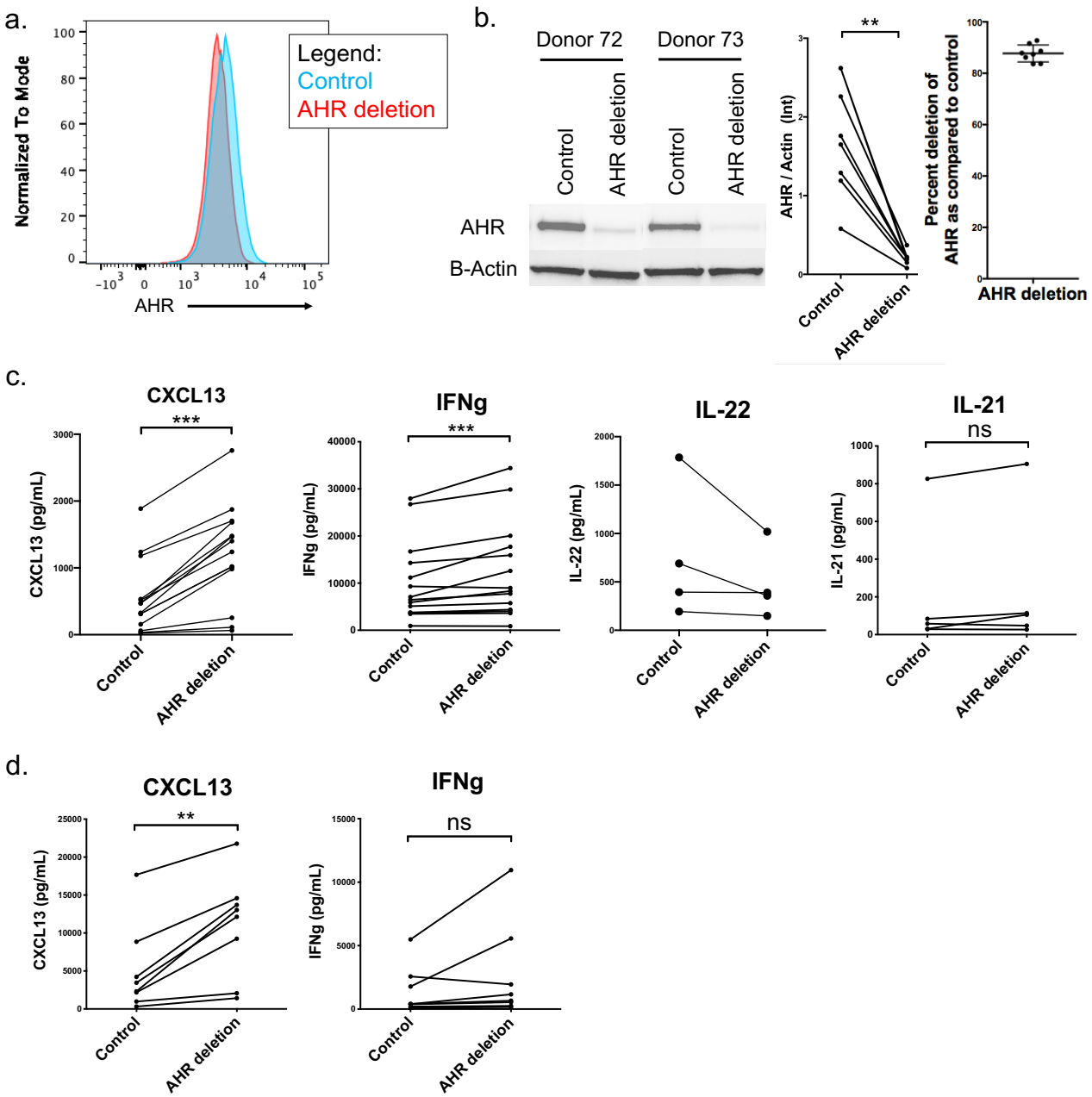

Figure 5. CRISPR deletion of AHR in human CD4$^+$ T cells and the effect on CXCL13, IFNγ, IL-2, and IL-21 at day 4 and CXCL13 and IFNγ at day 11. (a) Flow cytometry histogram of AHR expression in CD4$^+$ T cells for 1 donor when CRISPR edited with control (blue) and AHR guides (red) (b) Western blot assessment of AHR deletion for 2 separate donors and quantification of band intensity normalized to B-Actin for control (CD8) and AHR deletion. Percent deletion of AHR as compared to control for 8 donors calculated using western blot band intensity. (c) CXCL13, IFNγ, IL-22, and IL-21 ELISAs 4 days after electroporation; 14 donors for CXCL13 and IFNγ, 4 donors for IL-22, 6 donors for IL-21. (d) CXCL13 and IFNγ ELISAs 11 days after electroporation; 8 donors for CXCL13

and IFNγ. IL-21 and IL-22 was not detected at day 11. Each symbol represents a donor and error bars are standard deviations. Unless otherwise indicated, differences are not significant. Statistics: ns, not significant ($P > 0.05$); * $0.01<P < 0.05$; ** $0.001<P<0.01$; *** $0.0001<P<0.001$ (Wilcoxon signed rank test).

2.3.2.4 POU2F1

Preliminary analysis of RNA-seq data indicates that POU2F1 is more highly expressed in *ex vivo* Tph and *in vitro* differentiated Tph cells and may have a role in CXCL13 regulation as it is predicted to bind the CXCL13 promoter[63]. The data indicate that the deletion of POU2F1 was also successful, as determined by western blotting. Four guides against POU2F1 were used and all showed a decrease in POU2F1 expression as measured by western blotting **(Fig 6a)**. Guide #1 and #4 averaged a deletion efficiency of 50% in 2 donors. Guides #2 and #3 appeared to be most efficient as the deletion efficiency in 4 donors averaged at 65% and 62%, respectively **(Fig 6a)**. Four days after the electroporation with RNPs, the production of CXCL13 and IFNγ was not altered in all 4 guides when compared to control. This data indicate that POU2F1 is not an essential regulator of CXCL13 production in bulk human memory $CD4^+$ T cells from blood.

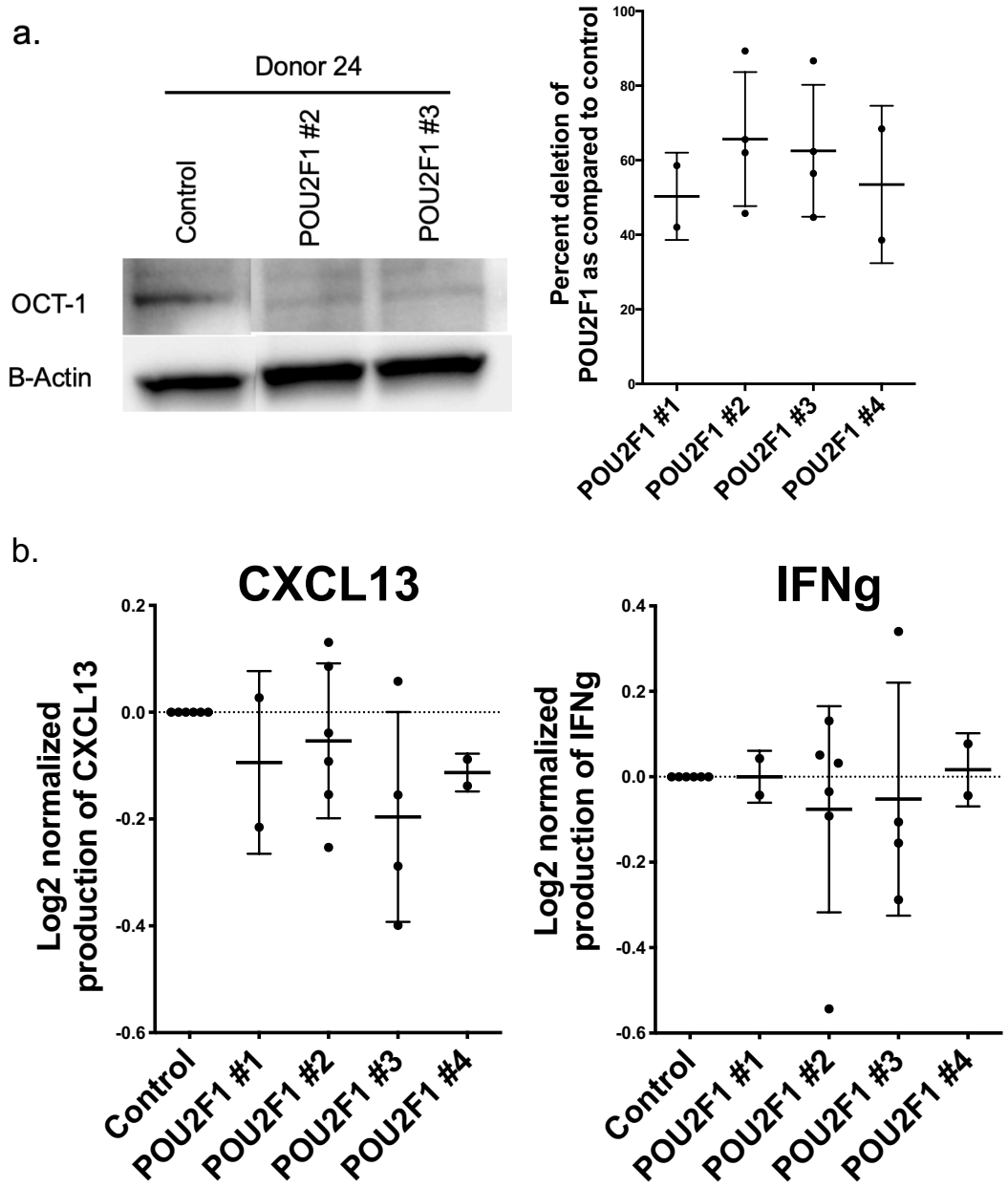

Figure 6. Deletion of POU2F1/OCT1 in human $CD4^+$ T cells and the effect on CXCL13 and IFNγ 4 days after electroporation. (a) Western blot analysis of POU2F1 deletion showing deletion using 2 guides in one donor. Percent deletion of POU2F1 as compared to control calculated using western blot band intensity; 4 donors for control, POU2F1 #2, and POU2F1 #3; 2 donors for POU2F1 #1 and POU2F1 #4. (b) CXCL13 and IFNγ ELISAs 4 days after electroporation; 4 donors for control, and POU2F1 #3; 6 donors for POU2F1 #2; 2 donors for POU2F1 #1 and POU2F1 #4. For the ELISAs, experimental conditions were normalized to control (CRISPR CD8) and the log base 2 of the standardized production of IFNγ and CXCL13 is plotted. Each symbol represents a donor and error bars are standard deviations. Unless otherwise indicated, differences are not significant.

2.3.2.5 RNF19A

Single cell RNA-seq analyses of RA synovial tissue indicated that RNF19A is the second most highly upregulated gene (after CXCL13) in synovial Tph cells as compared to other T cell subpopulations[5]. Using CRISPR we sought out to establish whether RNF19A deletion had an effect on CXCL13 production in $CD4^+$ T cells. We tested 4 guides against RNF19A in 2 donors and western blotting does not indicate that the protein level decreased 4 days after electroporation **(Fig 7a)**. We also tested the use of single guide RNAs (sgRNA) designed using the Broad Institute sgRNA designer (RNF19A #10 and RNF19A #11), but the protein levels of RNF19A remained unchanged **(Fig 7a)**. Using a multi-guide approach from Synthego in which 3 sgRNAs are combined together in order to form the RNP complexes, we tested varying Cas9/sgRNA ratios in 2 separate donors **(Fig 7b)**. The Synthego multi-guide approach did not alter protein expression as measured by western blotting. Additionally, the lack of abrogation of RNF19A expression was similar in the 2:1 sgRNA/Cas9 and 6:1 sgRNA/Cas9 ratios. DNA Sanger sequencing for guides #1-4 and analysis using TIDE (Tracking of Indels by Decomposition, Deskgen) revealed that 3 of the guides were able to induce InDels **(Fig 7c)**. The efficiency of the assay was not as high as anticipated as the highest average InDel frequency was around 38% for RNF19A #1 and the lowest was around 15% for RNF19A #2. Using RNF19A #4 the InDel frequency averaged 24.5% in 2 donors. DNA sequencing of cells electroporated with guide #3 was unsuccessful due to poor Sanger sequencing quality. The ability of the guides to alter *RNF19A* DNA sequence did not result in a significant decrease in protein expression **(Fig 7a)** or levels of RNF19A mRNA as measured by quantitative real-time PCR (RT-PCR) at day 4 and day 11 **(Fig 7d)**. Only guide #3 lowered the mRNA levels modestly at both time points as

compared to control. These results suggest that RNF19A was not efficiently edited out of human CD4$^+$ T cells. Further efforts will be required in order to establish a robust deletion of RNF19A.

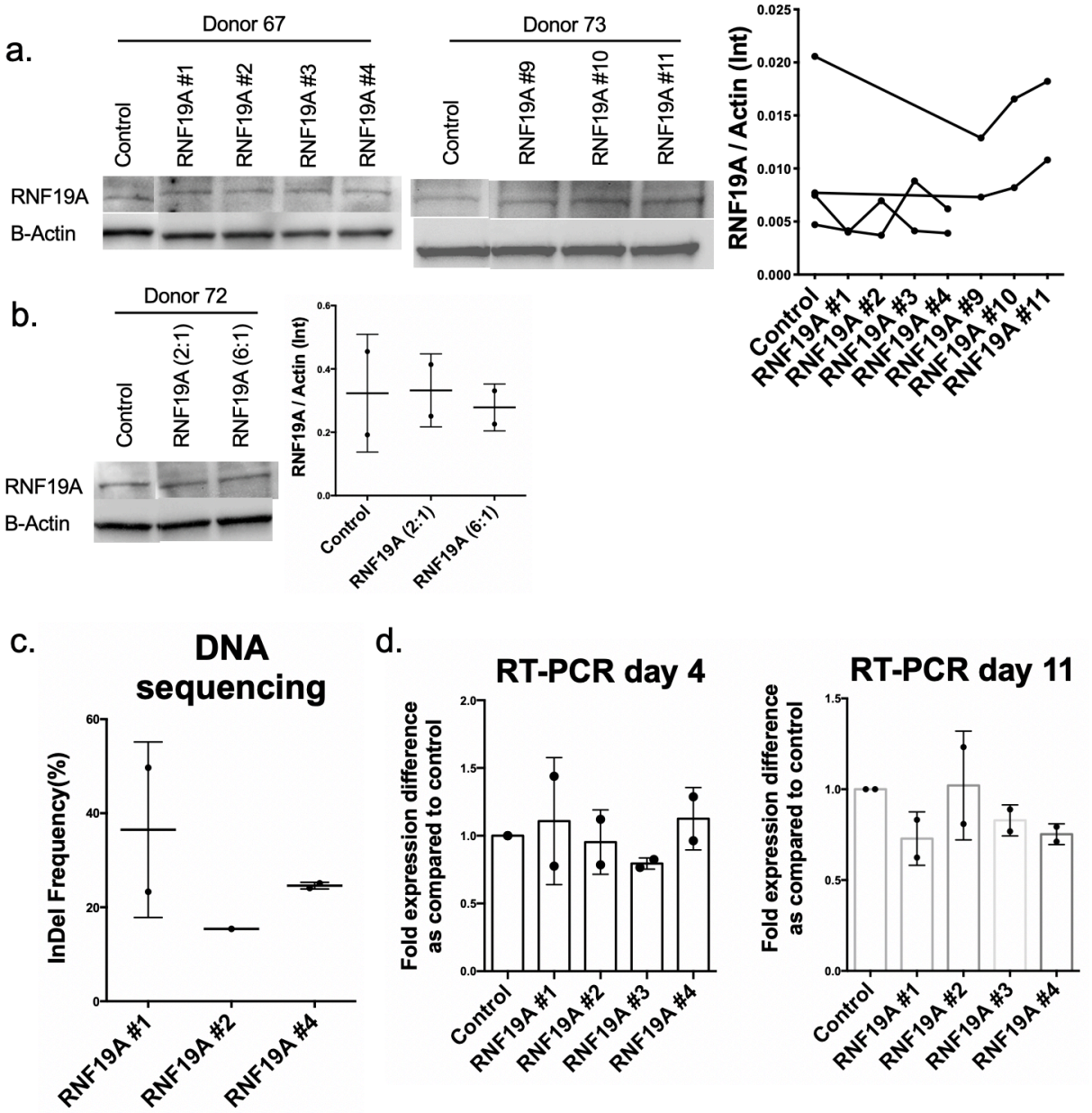

Figure 7. Deletion of RNF19A in human CD4$^+$ T cells 4 days after electroporation. (a) Western blot analysis of RNF19A deletion using 7 guides in 2 donors per guide. Quantification of RNF19A band intensity normalized to B-Actin for control (CD8) and the 7 RNF19A guides. (b) Western blot analysis of RNF19A deletion using Synthego's multi-guide approach. Quantification of RNF19A band intensity normalized to B-Actin for control (CD8) and RNF19A with 2:1 sgRNA/Cas9 ratio, and RNF19A with 6:1 sgRNA/Cas9 ratio. (c) Insertion/Deletion (InDel)

frequency based on DNA Sanger sequencing and calculated using TIDE (deskgen) for 3 guides; 2 donors for RNF19A #1 and RNF19A #3, 1 donor for RNF19A #2. (d) Real-Time quantitative PCR of cDNA from 2 donors 4 days post-electroporation and 2 donors 11 days post-electroporation with 4 RNF19A guides. Fold expression normalized to housekeeping gene RPL13A and calculated as $2^{-\Delta\Delta CT}$. Each symbol represents a donor and error bars are standard deviations. Unless otherwise indicated, differences are not significant.

After electroporation with RNF19A guides, CXCL13 and IFNγ was measured 4 days and 11 days post-electroporation. The use of guides 1-4 and 9-11 against RNF19A to electroporate $CD4^+$ T cells did not change the production of CXCL13 or IFNγ 4 days after electroporation **(Fig 8a)**. At day 4, only guide #11 modestly increased the levels of IFNγ. Using Synthego multi-guides targeting RNF19A, neither ratio of sgRNA/Cas9 altered secretion of CXCL13 or IFNγ **(Fig 8b)**. As a control we used the Synthego multi-guides against the T cell receptor alpha-chain (TRAC) which is part of the TCR complex and is required for adequate TCR signaling. As expected, the secretion of IFNγ was reduced by half while CXCL13 showed a downward trend **(Fig 8b)**. Eleven days after electroporation, CXCL13 and IFNγ production did not change when electroporated with RNF19A guides 1-4 as compared to control **(Fig 8c)**. The second guide appeared to increase the production of IFNγ modestly. Given that the deletion of RNF19A did not appear to be successful **(Fig 7)**, the role of RNF19A remains unclear in the production of CXCL13, and further work will be required to establish a robust deletion of RNF19A from $CD4^+$ T cells.

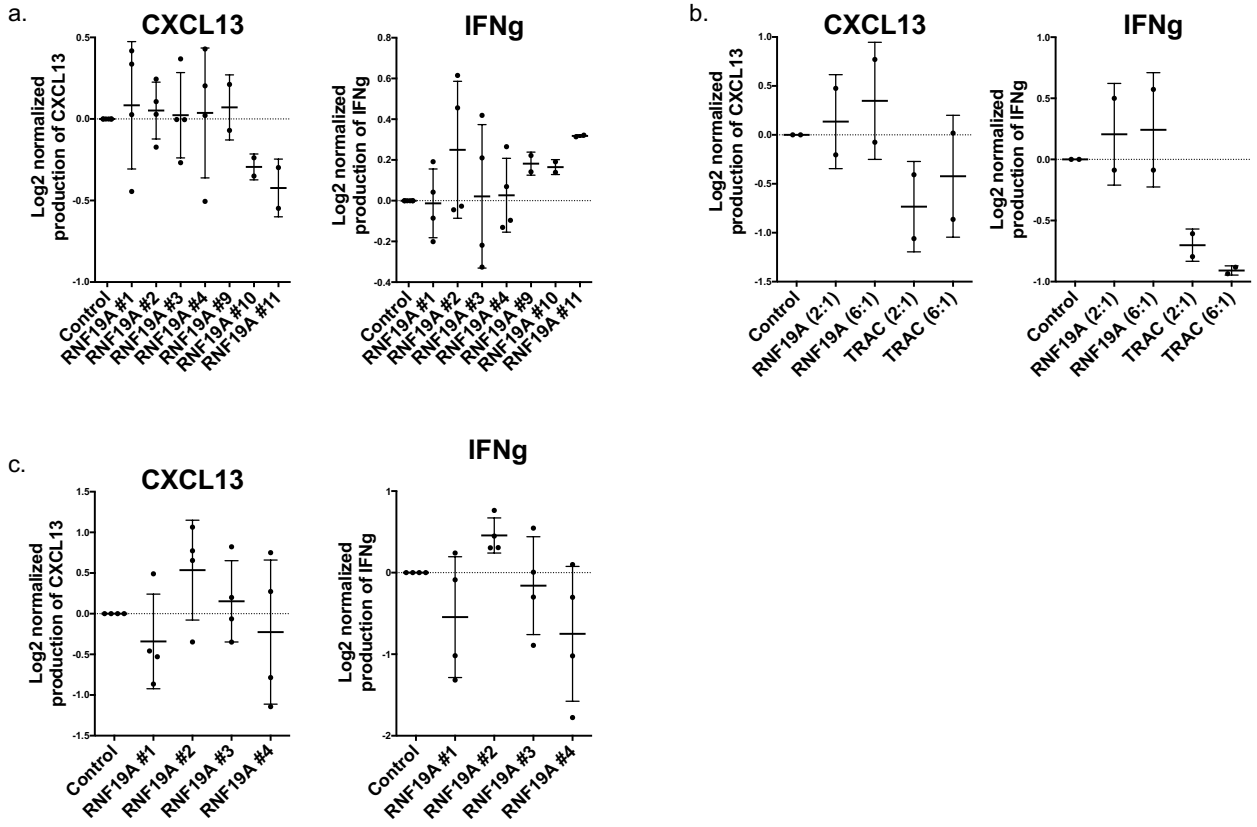

Figure 8. Effect of RNF19A deletion in $CD4^+$ T cells on CXCL13 production 4 days and 11 days after electroporation. (a) Four days after electroporation, CXCL13 and IFNγ secretion for 4 donors in guide 1-4 and 2 donors in guides 9-11. (b) At day 4, CXCL13 and IFNγ secretion for 2 donors using Synthego's multi-guide approach against RNF19A and T cell Receptor Alpha-Chain (TRAC). Varying sgRNA/Cas9 tested: 2:1 sgRNA/Cas9 ratio and 6:1 sgRNA/Cas9 ratio. (c) CXCL13 and IFNγ secretion at day 11 from 4 donors using guides 1-4. For the ELISAs, experimental conditions were normalized to control (CRISPR CD8) and the log base 2 of the standardized production of IFNγ and CXCL13 is plotted. Each symbol represents a donor and error bars are standard deviations. Unless otherwise indicated, differences are not significant.

Guide RNA	Type	DNA Sequence (5' → 3')	Designed with
AHR	gRNA	TCCCCTACTGAAAGAAACGG	DeskGen
MAF	gRNA	TGGAGATCTCCTGCTTGAGG	DeskGen
CD8	gRNA	TGTCGCCGCTGGATCGGACC	DeskGen
PD-1	gRNA	CGACTGGCCAGGGCGCCTGT	DeskGen
RNF19A #1	gRNA	ACCGCCAGCATGACTTCGGG	CHOPCHOP
RNF19A #2	gRNA	GTCGGAATCGCTTTAATAGC	CHOPCHOP
RNF19A #3	gRNA	GCTATTAAAGCGATTCCGAC	CHOPCHOP
RNF19A #4	gRNA	AAGGGAGCTAAATGGCGGGG	DeskGen
RNF19A #9	gRNA	AAATTAACTTGTGGGCGAGA	DeskGen
RNF19A #10	sgRNA	AATATCAAGCGAATATCATG	Broad
RNF19A #11	sgRNA	GTTGCCCAGAATGTACTGAA	Broad
RNF19A #13	sgRNA	AAGGGAGCTAAATGGCGGGG	Synthego
RNF19A #14	sgRNA	AAAAAAAGAAGAATTTCAAT	Synthego
RNF19A #15	sgRNA	ATGAGTTTACATCGGCAAAT	Synthego
SOX4 #1	gRNA	ATCCTGCATAGCCCAAACAG	DeskGen
SOX4 #2	gRNA	AAGCGCGTCTACCTGTTCGG	CHOPCHOP
SOX4 #3	gRNA	CGACCACCACTCGCTGTACA	CHOPCHOP
SOX4 #4	gRNA	TCCGCGCCTTGTACAGCGAG	CHOPCHOP
SOX4 #5	sgRNA	CAAGATCCCTTTCATTCGAG	Broad
SOX4 #7	sgRNA	AAAGAGCTGCGGCTCCAAAG	Broad
BCL6 #1	gRNA	GACATCCCGAAACTCCTCAT	CHOPCHOP
BCL6 #2	gRNA	TCCTCATAAGCAGAGCGTCT	DeskGen
BCL6 #3	gRNA	GTTCCGGTTCGAGGCTCGAG	DeskGen
BCL6 #4	gRNA	CACCACCTCACGACCCCGAT	IDT
POU2F1 #1	gRNA	TACTTATAGGTCCAACTCGC	DeskGen
POU2F1 #2	gRNA	ACTCGCTGGAACAAGTTTAC	DeskGen
POU2F1 #3	gRNA	ATATTCAAAATGGCGGACGG	DeskGen
POU2F1 #4	gRNA	AAAATATTCAAAATGGCGGA	DeskGen
TRAC #1	sgRNA	CTCTCAGCTGGTACACGGCA	Synthego
TRAC #2	sgRNA	GAGAATCAAAATCGGTGAAT	Synthego
TRAC #3	sgRNA	ACAAAACTGTGCTAAGACATG	Synthego

Table 1. Guide RNAs used for CRISPR/Cas9 RNP complexes. Types of guide RNAs, sequences, program used to design each of them is illustrated in the table above.

2.4 Summary:

The data suggest that electroporation of RNPs in $CD4^+$ T cells is a highly efficient way of knocking out genes using CRISPR/Cas9 as noted by the deletion of PD-1 **(Fig 1),** MAF **(Fig 2)**, BCL6 **(Fig 3)**, AHR **(Fig 5)**, and POU2F1 **(Fig 6)**. CRISPR deletion of MAF decreased the

production of IL-21 while not changing CXCL13 levels. A known regulator of Tfh cells, BCL6, was confirmed to promote CXCL13 production **(Fig 4)**. AHR proved to be a strong negative regulator of CXCL13 in $CD4^+$ T cells as deletion of AHR increased CXCL13 production robustly **(Fig 5)**. Of the other targets, we did not observe effects of loss of POU2F1 on CXCL13 production **(Fig 6),** and interrogation of RNF19A and SOX4 require further method development.

Chapter 3: Discussion and Perspective

Chronically inflamed tissues may develop pathogenic T cell – B cell lymphoid aggregates capable of producing antibodies in the periphery[3]. The T cell – B cell interactions are carefully and tightly regulated by key cytokines such as CXCL13[2]. In humans, CXCL13 is produced mainly by Tfh and Tph cells to help recruit B cells[1,20] but as of now, the regulation of CXCL13 in $CD4^+$ T cells is not entirely understood. CXCL13 regulation is of particular interest in RA as CXCL13 helps in the formation of pathogenic T-B cell aggregates through the recruitment of immune cells expressing its receptor CXCR5 and may develop further into ectopic lymphoid organs. These aggregates can then lead to more erosive and severe disease[6,13,30]. The principal source of CXCL13 in the synovium are Tph cells[5,35]. In the periphery, Tph cells are able to help B cells differentiate into plasma cells and produce antibodies as they secrete IL-21 and CXCL13[20,21]. Therefore, concretizing how CXCL13 production is controlled in $CD4^+$ T cells may prove valuable in mitigating disease course and lead to potential treatment options. In particular, targeting potent regulators of CXCL13 in Tph cells may impair pathogenic mechanisms while leaving homeostatic immune functions intact in other cell types. Some transcription factors such as BCL6 and SOX4 have been implicated in regulating CXCL13 in human $CD4^+$ T cells[18,41]. In addition, CyTOF and RNAseq data of Tph cells revealed multiple new potential CXCL13 regulators. Here we chose to focus on three selected targets: AHR, POU2F1, and RNF19A. Using CRISPR/Cas9, we electroporated RNP complexes directly inside $CD4^+$ T cells to delete targets of interests. We then assessed the effect of the deletion on CXCL13 production.

Upon CRISPR deletion of PD-1 using RNP electroporation, PD-1 cell surface expression decreased by > 90% in 4 donors **(Fig 1)**. The efficiency is on par with other research groups

using RNP electroporation to CRISPR edit $CD4^+$ T cells . Additionally, we were able to reproduce data published by our group[21] showing that CRISPR deletion of MAF decreased the production of IL-21 from $CD4^+$ T cells **(Fig 2)**. However, deletion of MAF did not affect CXCL13 production. This indicates that distinct transcription factors are important for different Tph/Tfh functions and that multiple factors act in concert to regulate the Tph/Tfh cellular program.

The master Tfh transcription factor has also been implicated in the production of CXCL13 as lentiviral overexpression of BCL6 in $CXCR5^{int}$ Tfh cells increased CXCL13 secretion[18]. Tph cells, however, express low levels of BCL6 and yet, they secrete large amounts of CXCL13[20]. This suggests that BCL6 may not be an essential driver of CXCL13. Our data suggest that deletion of BCL6 using guide #4 decreased CXCL13 while not affecting IFNγ production from memory $CD4^+$ T cells **(Fig 3)**. Contrary to our hypothesis, this confirms that BCL6 is a positive regulator of CXCL13, as previously indicated in the literature[18]. Tfh cells express high levels of BCL6 and CXCL13 while Tph cells do not express comparable levels of BCL6 and yet produce large amounts of CXCL13[3]. This discrepancy may be explained by the presence of multiple regulators present in different cell types; the regulation of CXCL13 in Tph cells may distinct from that of Tfh cells. Additionally, it may also indicate that low levels of BCL6 are sufficient to induce CXCL13 in $CD4^+$ T cells. Overall, the data help establish BCL6 as a positive regulator of CXCL13 in $CD4^+$ T cells.

SOX4 is one of the published positive CXCL13 regulators as it was found to be essential in differentiating CXCL13-producing $CD4^+$ T cells[41]. CRISPR deletion of SOX4 proved to be challenging and appears to have been unsuccessful as measured by western blotting **(Fig 4)**. We first attempted to use 4 RNA guides designed with 2 separate programs (CHOPCHOP and

Deskgen) but none resulted in deletion of SOX4. We tested the use of 2 single RNA guides designed with the Broad's sgRNA designer, which can be ligated to Cas9 directly as they already contain both crRNA and trRNA components, and both guides did not result in a decrease of SOX4 expression. Additionally, three primary antibodies against SOX4 were tested to find the most specific antibodies and we concluded that the abcam anti-SOX4 antibody was the most specific as the highest intensity band was at the expected molecular weight of SOX4 and the number of non-specific bands was lower than other antibodies. However, the use of either antibodies did not indicate that any of the 6 guides decreased the expression of SOX4. In the future, it will be essential to collect DNA sequencing data in order to establish whether the guides are inducing InDels within the *SOX4* gene. Additionally, a T7 endonuclease assay could be performed to establish the efficiency of the guides in editing *SOX4.* In a T7 endonuclease assay, depending on whether editing has occurred, more mismatched DNA will be present in the PCR product. The T7 endonuclease then cleaves mismatched DNA and more bands appear when the PCR product is run on a DNA gel.

We may also have to consider other alternatives to western blotting, such as measuring SOX4 RNA levels through RT-PCR. In order to establish whether deletion can be detected at a later time point, cell lysates will be collected 11 days after electroporation. The half-life of SOX4 may be too long to detect deletion 4 days after electroporation. As protein turnover would be hindered by the induction of InDels in *SOX4*, SOX4 protein levels would not be able to be replenished and decreased levels would be detectable after 11 days. Yoshitomi *et al.*'s research indicates that SOX4 is important in the differentiation of naïve $CD4^+$ T cells to CXCL13-producing T cells[41]. If deletion of SOX4 decreases the production of CXCL13 from memory $CD4^+$ T cells, this would indicate that SOX4 is not only involved in differentiation but is also

necessary for continued production of CXCL13 after differentiation. On the contrary, if SOX4 deletion does not affect CXCL13 production in memory $CD4^+$ T cells, this would indicate that SOX4 is not crucial in driving CXCL13 production past differentiation. Overall, our data suggest that SOX4 deletion was unsuccessful and more efforts need to be made in order to establish the deletion of SOX4.

AHR expression level was higher in Tph and Tfh cells as compared to PD-1^- and naïve $CD4^+$ T cells, as determined by CyTOF of $CD4^+$ T cells from RA, SLE, and control patients (data not shown). The lab had previously noted that treatment of $CD4^+$ T cells with AHR agonist, TCDD, decreased the production of CXCL13. On the contrary, treatment with AHR antagonist CH-22 increased CXCL13 production (data not shown). Here, we report that deletion of AHR was highly efficient and successful as noted by western blotting and increased the production of CXCL13 by more than 3-fold **(Fig 5)**. The effect of the deletion was mostly confined to CXCL13 as production of IL-21 and IFNγ did not change. This indicates that AHR may be responsible for some functions of Tph/Tfh cells by negatively regulating CXCL13 while not affecting other functions (ie. IL-21). This brings up an apparent paradox: why would Tph/Tfh cells express increased levels of AHR if AHR functions as an inhibitor of their function? As opposed to the total AHR expression level, the level of AHR activation in T cells may be more critical. Activation of AHR may be low in Tph/Tfh cells due to the concentration of AHR agonists/antagonists within their niche. The high expression of AHR in Tph/Tfh cells may poise cells to inhibit CXCL13 secretion upon increased concentration of AHR ligands. This may be a protective mechanism by which alteration of AHR ligand concentrations can mitigate the exacerbation of inflammation and activation of humoral immunity. Past literature revealed that stimulation of human naïve $CD4^+$ T cells with IL-2 and AHR agonist TCDD did not change the

expression of BCL6[51]. Our data suggest the same: CRISPR deletion of AHR did not decrease the percent of BCL6 positive cells as measured through flow cytometry (data not shown). This would indicate that AHR does not regulate known regulators of Tph function, but rather, it regulates transcription directly or influences other uncovered regulators. Although AHR can bind DNA upon activation, AHR was also shown to have E3 ubiquitin ligase activity[48] and may participate in CXCL13 regulation by targeting positive regulators for proteasomal degradation upon activation. It will be interesting in the future to assess how AHR activation influence the proteomic and transcriptional landscape within $CD4^+$ T cells in order to elucidate its mechanism of action. Although AHR's mechanism remains unknown, this data establish AHR as a strong negative regulator of CXCL13 in $CD4^+$ T cells.

Of the potential CXCL13 regulator candidates, POU2F1/OCT-1 was of particular interest for its ability to help POU2AF1 bind DNA. POU2AF1 was most highly expressed in Tph cells compared to other cell types and OCT-1 is predicted to bind the CXCL13 promoter[63]. Our data suggest that OCT-1 does not play an essential role in regulating CXCL13 in $CD4^+$ T cells as deletion did not affect CXCL13 secretion **(Fig 6)**. As both OCT-1 and OCT-2 help POU2AF1 bind to DNA, the role of OCT-1 and OCT-2 in regulating CXCL13 production may be redundant in $CD4^+$ T cells. Even though OCT-2 is more highly expressed in B cells[57], OCT-2 is also expressed in T cells, albeit at low levels[75]. In mice, T cell stimulation was shown to induce Oct-2 expression[76]. It is possible that the deletion of OCT-1 may shift the balance towards the use OCT-2 in $CD4^+$ T cells and therefore, deletion of OCT-1 may not affect POU2AF1's ability to bind the CXCL13 promoter as it may associate with OCT-2[57]. Past groups reported that $Pou2af1^{-/-}$ Tfh cells showed a decreased expression of Bcl6 compared to WT Tfh cells as Pou2af1 could bind the Bcl6 promoter with the help of Oct-1 and Oct-2[62]. Since BCL6 was

indicated to be a positive regulator of CXCL13 **(Fig 4)**, POU2AF1 may influence CXCL13 production by regulating BCL6 expression. Deletion of POU2AF1 will be important to perform in future experiments in order to establish whether POU2AF1 has a role in CXCL13 production.

RNA-sequencing analysis revealed that RNF19A, an E3 ubiquitin ligase, was the second most differentially expressed gene in Tph cells compared to other RA synovial immune cells (data not shown). CRISPR deletion of RNF19A was particularly challenging and did not seem to work **(Fig 7)**. Electroporation with 5 guide RNAs and 2 single guide RNAs designed with multiple programs did not result in the loss of expression as measured by western blotting. Using Synthego's multi-guide approach, which combines 3 single guide RNAs together, RNF19A expression remained strong. Additionally, 3 guides out 4 did not alter RNF19A mRNA levels and only 1 guide showed a modest decrease in RNF19A mRNA. DNA sequencing data for 3 guides indicated that InDels were induced within the *RNF19A* gene with varying frequency ranging from 15% to 50% depending on the guide and donor. However, the frequency of InDel induction does not seem to be sufficient to affect protein or mRNA levels. In order to establish the InDel efficiency of the other guides, more DNA sequencing data will need to be collected. Additionally, protein levels will be assessed at later time points (ie. 11 days post-electroporation) in case the RNF19A protein half-life is too long to detect protein loss 4 days post-electroporation. Once deletion of RNF19A is established, it will be essential to determine which proteins it targets for proteasomal degradation using quantitative proteomics analysis. RNF19A was reported to ubiquitinylate and tag TRAF6 for proteasomal degradation[67], but the use RNF19A guides 1-4 did not decrease TRAF6 expression as assessed by western blotting (data not shown). Once the efficiencies of the guides are established, TRAF6 expression will need to

be re-assessed. Altogether, more efforts need to be made to delete RNF19A from $CD4^+$ T cells in order to establish its role in CXCL13 regulation.

Drawbacks of this study include the use of sorted memory $CD4^+$ T cells, whose regulation of CXCL13 may not fully mirror CXCL13 regulation in Tph cells within the synovium. For instance, RNF19A was shown to require the NOD-like Receptor NLRP11 to ubiquitinylate TRAF6[67]. The expression of assistive proteins such as NLRP11 in Tph cells compared to sorted memory $CD4^+$ T cells may differ and thus regulation of the transcriptomic and proteomic landscape can in turn be quite distinct. Additionally, decreases in CXCL13 upon deletion of BCL6 from memory $CD4^+$ T cells may only reflect effects attributed to BCL6-expressing Tfh cells. To test whether BCL6 is essential to Tph CXCL13 regulation, sorted Tph will need to be edited. As a whole, one of the critical next steps is to delete factors of interest in sorted Tph cells from RA patients. Additionally, the deletion of other factors needs to be assessed and can be done using CRISPR screens, which can target a multitude of candidates efficiently.

The CRISPR deletion of RNF19A and SOX4 proved to be challenging and will, therefore, need to be revisited. First the effect of electroporation at later time points need to be assessed to determine whether protein half-life is a contributing factor in the continued expression of RNF19A and SOX4. If protein expression is not altered, other possible methods include post-transcriptional gene silencing through the use of small interfering RNAs (siRNA) specific for RNF19A and SOX4 mRNAs. CRISPR was originally used because less off-targets effects are observed when compared to the use of siRNA[77] and siRNA only serve to "knockdown" protein expression rather than "knockout" protein levels. However, these targets may require a different approach. Assessing the efficiency of deletion can be problematic as

commercially available antibodies against RNF19A and SOX4 are polyclonal and the resulting western blots are difficult to interpret. Additionally, since CRISPR editing of *RNF19A* and *SOX4* genes may not alter RNA levels, the efficiency of deletion is difficult to establish through RT-PCR. Successful gene silencing using siRNA would alter RNA levels and knockdown efficiency would be more easily assessed through RT-PCR.

The CRISPR deletion of POU2F1 was successful but did not influence CXCL13 production. This may be due to redundant roles of OCT-1 and OCT-2. In the future, POU2AF1 will need to be deleted to elucidate any regulatory role it may have on CXCL13. Furthermore, understanding the mechanism through which AHR influences CXCL13 production will be important. Whether AHR influences CXCL13 transcription directly or influences other factors remains unknown. Additionally, future work evaluating whether other B cell helper function are controlled by AHR will be beneficial. In the synovium, the concentrations of AHR ligands/inhibitors remain unclear and will need to be assessed in order to link CXCL13 production from synovial Tph cells to decreased AHR activity. The use of AHR agonists in treatment of RA as to limit the production of CXCL13 from Tph cells within the synovium may not be a viable treatment as it may exacerbate Th17 response[55,56]. Therefore more efforts need to be made to selectively modify AHR activity within Tph cells.

Overall, the data establish AHR as a novel negative regulator of CXCL13 and BCL6 as a positive regulator of CXCL13. These may prove to be significant targets in preventing the development of pathogenic T-B aggregates in RA synovium and could potentially be used to mitigate disease course.

References

1. Crotty, S. Follicular Helper CD4 T Cells (TFH). *Annu. Rev. Immunol.* **29**, 621–663 (2011).

2. Stebegg, M. *et al.* Regulation of the Germinal Center Response. *Front. Immunol.* **9**, (2018).

3. Rao, D. A. T Cells That Help B Cells in Chronically Inflamed Tissues. *Front. Immunol.* **9**, (2018).

4. Smolen, J. S. *et al.* Rheumatoid arthritis. *Nat. Rev. Dis. Primer* **4**, 1–23 (2018).

5. Zhang, F. *et al.* Defining inflammatory cell states in rheumatoid arthritis joint synovial tissues by integrating single-cell transcriptomics and mass cytometry. *Nat. Immunol.* **20**, 928–942 (2019).

6. Klimiuk, P. A., Goronzy, J. J., Björ nsson, J., Beckenbaugh, R. D. & Weyand, C. M. Tissue cytokine patterns distinguish variants of rheumatoid synovitis. *Am. J. Pathol.* **151**, 1311–1319 (1997).

7. Takemura, S. *et al.* Lymphoid Neogenesis in Rheumatoid Synovitis. *J. Immunol.* **167**, 1072–1080 (2001).

8. Holers, V. M. Autoimmunity to Citrullinated Proteins and the Initiation of Rheumatoid Arthritis. *Curr. Opin. Immunol.* **25**, 728–735 (2013).

9. Humby, F. *et al.* Ectopic Lymphoid Structures Support Ongoing Production of Class-Switched Autoantibodies in Rheumatoid Synovium. *PLOS Med.* **6**, e1 (2009).

10. Aletaha, D., Alasti, F. & Smolen, J. S. Rheumatoid factor, not antibodies against citrullinated proteins, is associated with baseline disease activity in rheumatoid arthritis clinical trials. *Arthritis Res. Ther.* **17**, 229 (2015).

11. Nielen, M. M. J. *et al.* Antibodies to citrullinated human fibrinogen (ACF) have diagnostic and prognostic value in early arthritis. *Ann. Rheum. Dis.* **64**, 1199–1204 (2005).

12. Rosengren, S. *et al.* Elevated autoantibody content in rheumatoid arthritis synovia with lymphoid aggregates and the effect of rituximab. *Arthritis Res. Ther.* **10**, R105 (2008).

13. Klimiuk, P. A. *et al.* Serum cytokines in different histological variants of rheumatoid arthritis. *J. Rheumatol.* **28**, 1211–1217 (2001).

14. Ettinger, R. *et al.* IL-21 Induces Differentiation of Human Naive and Memory B Cells into Antibody-Secreting Plasma Cells. *J. Immunol.* **175**, 7867–7879 (2005).

15. Yu, M., Cavero, V., Lu, Q. & Li, H. Follicular helper T cells in rheumatoid arthritis. *Clin. Rheumatol.* **34**, 1489–1493 (2015).

16. Nurieva, R. I. *et al.* Bcl6 Mediates the Development of T Follicular Helper Cells. *Science* **325**, 1001–1005 (2009).

17. Johnston, R. J. *et al.* Bcl6 and Blimp-1 Are Reciprocal and Antagonistic Regulators of T Follicular Helper Cell Differentiation. *Science* **325**, 1006–1010 (2009).

18. Kroenke, M. A. *et al.* Bcl6 and Maf Cooperate To Instruct Human Follicular Helper CD4 T Cell Differentiation. *J. Immunol.* **188**, 3734–3744 (2012).

19. Ma, J. *et al.* Increased Frequency of Circulating Follicular Helper T Cells in Patients with Rheumatoid Arthritis. *Clinical and Developmental Immunology* vol. 2012 e827480 https://www.hindawi.com/journals/jir/2012/827480/ (2012).

20. Rao, D. A. *et al.* Pathologically expanded peripheral T helper cell subset drives B cells in rheumatoid arthritis. *Nature* **542**, 110–114 (2017).

21. Bocharnikov, A. V. *et al.* PD-1^{hi}CXCR5^{-} T peripheral helper cells promote B cell responses in lupus via MAF and IL-21. *JCI Insight* **4**, (2019).

22. Hiramatsu, Y. *et al.* c-Maf activates the promoter and enhancer of the IL-21 gene, and TGF-β inhibits c-Maf-induced IL-21 production in CD4+ T cells. *J. Leukoc. Biol.* **87**, 703–712 (2010).

23. Gu-Trantien, C. *et al.* CXCL13-producing T_{FH} cells link immune suppression and adaptive memory in human breast cancer. *JCI Insight* **2**, (2017).

24. Singh, D. *et al.* CD4+ follicular helper-like T cells are key players in anti-tumor immunity. *bioRxiv* 2020.01.08.898346 (2020) doi:10.1101/2020.01.08.898346.

25. Liu Lufang *et al.* Endothelial Cell-Derived IL-18 Released During Ischemia Reperfusion Injury Selectively Expands T Peripheral Helper Cells to Promote Alloantibody Production. *Circulation* **0**,.

26. Renand, A. *et al.* Integrative molecular profiling of autoreactive CD4 T cells in autoimmune hepatitis. *bioRxiv* 2020.01.06.895938 (2020) doi:10.1101/2020.01.06.895938.

27. Kazanietz, M. G., Durando, M. & Cooke, M. CXCL13 and Its Receptor CXCR5 in Cancer: Inflammation, Immune Response, and Beyond. *Front. Endocrinol.* **10**, (2019).

28. Follicular stromal cells and lymphocyte homing to follicles. *Immunol. Rev.* **176**, 181–193 (2000).

29. Shi, K. *et al.* Lymphoid Chemokine B Cell-Attracting Chemokine-1 (CXCL13) Is Expressed in Germinal Center of Ectopic Lymphoid Follicles Within the Synovium of Chronic Arthritis Patients. *J. Immunol.* **166**, 650–655 (2001).

30. Bugatti, S. *et al.* High expression levels of the B cell chemoattractant CXCL13 in rheumatoid synovium are a marker of severe disease. *Rheumatology* **53**, 1886–1895 (2014).

31. Luther, S. A., Lopez, T., Bai, W., Hanahan, D. & Cyster, J. G. BLC Expression in Pancreatic Islets Causes B Cell Recruitment and Lymphotoxin-Dependent Lymphoid Neogenesis. *Immunity* **12**, 471–481 (2000).

32. Dennis, G. *et al.* Synovial phenotypes in rheumatoid arthritis correlate with response to biologic therapeutics. *Arthritis Res. Ther.* **16**, R90 (2014).

33. Greisen, S. R. *et al.* CXCL13 predicts disease activity in early rheumatoid arthritis and could be an indicator of the therapeutic 'window of opportunity'. *Arthritis Res. Ther.* **16**, (2014).

34. Meeuwisse, C. M. *et al.* Identification of CXCL13 as a marker for rheumatoid arthritis outcome using an in silico model of the rheumatic joint. *Arthritis Rheum.* **63**, 1265–1273 (2011).

35. Stephenson, W. *et al.* Single-cell RNA-seq of rheumatoid arthritis synovial tissue using low-cost microfluidic instrumentation. *Nat. Commun.* **9**, 1–10 (2018).

36. Thurlings, R. M. *et al.* Synovial lymphoid neogenesis does not define a specific clinical rheumatoid arthritis phenotype. *Arthritis Rheum.* **58**, 1582–1589 (2008).

37. Sande, M. G. H. van de *et al.* Presence of lymphocyte aggregates in the synovium of patients with early arthritis in relationship to diagnosis and outcome: is it a constant feature over time? *Ann. Rheum. Dis.* **70**, 700–703 (2011).

38. Manzo, A. *et al.* Systematic microanatomical analysis of CXCL13 and CCL21 in situ production and progressive lymphoid organization in rheumatoid synovitis. *Eur. J. Immunol.* **35**, 1347–1359 (2005).

39. Kobayashi, S. *et al.* TGF-β induces the differentiation of human CXCL13-producing CD4+ T cells. *Eur. J. Immunol.* **46**, 360–371 (2016).

40. Locci, M. *et al.* Activin A programs the differentiation of human T FH cells. *Nat. Immunol.* **17**, 976–984 (2016).

41. Yoshitomi, H. *et al.* Human Sox4 facilitates the development of CXCL13-producing helper T cells in inflammatory environments. *Nat. Commun.* **9**, 1–10 (2018).

42. Schilham, M. W., Moerer, P., Cumano, A. & Clevers, H. C. Sox-4 facilitates thymocyte differentiation. *Eur. J. Immunol.* **27**, 1292–1295 (1997).

43. Kuwahara, M. *et al.* The transcription factor Sox4 is a downstream target of signaling by the cytokine TGF-β and suppresses T H 2 differentiation. *Nat. Immunol.* **13**, 778–786 (2012).

44. Nancy Garrick, D. D. Accelerating Medicines Partnership (AMP). *National Institute of Arthritis and Musculoskeletal and Skin Diseases* https://www.niams.nih.gov/grants-funding/funded-research/accelerating-medicines (2017).

45. Rothhammer, V. & Quintana, F. J. The aryl hydrocarbon receptor: an environmental sensor integrating immune responses in health and disease. *Nat. Rev. Immunol.* **19**, 184–197 (2019).

46. Durrin, L. K., Jones, P. B. C., Fisher, J. M., Galeazzi, D. R. & Whitlock, J. P. 2,3,7,8-Tetrachlorodibenzo-p-dioxin receptors regulate transcription of the cytochrome P1-450 gene. *J. Cell. Biochem.* **35**, 153–160 (1987).

47. Gutiérrez-Vázquez, C. & Quintana, F. J. Regulation of the Immune Response by the Aryl Hydrocarbon Receptor. *Immunity* **48**, 19–33 (2018).

48. Ohtake, F. *et al.* Dioxin receptor is a ligand-dependent E3 ubiquitin ligase. *Nature* **446**, 562–566 (2007).

49. Kerkvliet, N. I. *et al.* Role of the Ah locus in suppression of cytotoxic T lymphocyte activity by halogenated aromatic hydrocarbons (PCBs and TCDD): Structure-activity relationships and effects in C57Bl6 mice congenic at the Ah locus. *Fundam. Appl. Toxicol.* **14**, 532–541 (1990).

50. Funatake, C. J., Marshall, N. B., Steppan, L. B., Mourich, D. V. & Kerkvliet, N. I. Cutting Edge: Activation of the Aryl Hydrocarbon Receptor by 2,3,7,8-Tetrachlorodibenzo-p-dioxin Generates a Population of CD4+CD25+ Cells with Characteristics of Regulatory T Cells. *J. Immunol.* **175**, 4184–4188 (2005).

51. Goettel, J. A. *et al.* AHR Activation Is Protective against Colitis Driven by T Cells in Humanized Mice. *Cell Rep.* **17**, 1318–1329 (2016).

52. Gandhi, R. *et al.* Activation of the aryl hydrocarbon receptor induces human type 1 regulatory T cell–like and Foxp3 + regulatory T cells. *Nat. Immunol.* **11**, 846–853 (2010).

53. Apetoh, L. *et al.* The aryl hydrocarbon receptor interacts with c-Maf to promote the differentiation of type 1 regulatory T cells induced by IL-27. *Nat. Immunol.* **11**, 854–861 (2010).

54. Ramirez, J.-M. *et al.* Activation of the aryl hydrocarbon receptor reveals distinct requirements for IL-22 and IL-17 production by human T helper cells. *Eur. J. Immunol.* **40**, 2450–2459 (2010).

55. Veldhoen, M. *et al.* The aryl hydrocarbon receptor links T H 17-cell-mediated autoimmunity to environmental toxins. *Nature* **453**, 106–109 (2008).

56. Veldhoen, M., Hirota, K., Christensen, J., O'Garra, A. & Stockinger, B. Natural agonists for aryl hydrocarbon receptor in culture medium are essential for optimal differentiation of Th17 T cells. *J. Exp. Med.* **206**, 43–49 (2009).

57. Teitell, M. A. OCA-B regulation of B-cell development and function. *Trends Immunol.* **24**, 546–553 (2003).

58. Qin, X.-F., Reichlin, A., Luo, Y., Roeder, R. G. & Nussenzweig, M. C. OCA-B integrates B cell antigen receptor-, CD40L- and IL 4-mediated signals for the germinal center pathway of B cell development. *EMBO J.* **17**, 5066–5075 (1998).

59. Brunner, C. *et al.* BOB.1/OBF.1 controls the balance of TH1 and TH2 immune responses. *EMBO J.* **26**, 3191–3202 (2007).

60. Shakya, A. *et al.* Oct1 and OCA-B are selectively required for CD4 memory T cell function. *J. Exp. Med.* **212**, 2115–2131 (2015).

61. Yamashita, K. *et al.* POU2AF1 arranges systemic distribution of follicular helper T cells (IRC10P.466). *J. Immunol.* **192**, 192.4-192.4 (2014).

62. Stauss, D. *et al.* The transcriptional coactivator Bob1 promotes the development of follicular T helper cells via Bcl6. *EMBO J.* **35**, 881–898 (2016).

63. CXCL13 Gene - GeneCards | CXL13 Protein | CXL13 Antibody. https://www.genecards.org/cgi-bin/carddisp.pl?gene=CXCL13.

64. Hu, X. *et al.* Integrating Autoimmune Risk Loci with Gene-Expression Data Identifies Specific Pathogenic Immune Cell Subsets. *Am. J. Hum. Genet.* **89**, 496–506 (2011).

65. Zheng, N. & Shabek, N. Ubiquitin Ligases: Structure, Function, and Regulation. *Annu. Rev. Biochem.* **86**, 129–157 (2017).

66. Akutsu, M., Dikic, I. & Bremm, A. Ubiquitin chain diversity at a glance. *J. Cell Sci.* **129**, 875–880 (2016).

67. Wu, C. *et al.* NLRP11 attenuates Toll-like receptor signalling by targeting TRAF6 for degradation via the ubiquitin ligase RNF19A. *Nat. Commun.* **8**, 1–15 (2017).

68. Shi, J.-H. & Sun, S.-C. Tumor Necrosis Factor Receptor-Associated Factor Regulation of Nuclear Factor κB and Mitogen-Activated Protein Kinase Pathways. *Front. Immunol.* **9**, (2018).

69. Juilland, M. & Thome, M. Holding All the CARDs: How MALT1 Controls CARMA/CARD-Dependent Signaling. *Front. Immunol.* **9**, (2018).

70. Motegi, H., Shimo, Y., Akiyama, T. & Inoue, J. TRAF6 negatively regulates the Jak1-Erk pathway in interleukin-2 signaling. *Genes Cells* **16**, 179–189 (2011).

71. Doudna, J. A. & Charpentier, E. The new frontier of genome engineering with CRISPR-Cas9. *Science* **346**, (2014).

72. Seki, A. & Rutz, S. Optimized RNP transfection for highly efficient CRISPR/Cas9-mediated gene knockout in primary T cells. *J. Exp. Med.* **215**, 985–997 (2018).

73. Schumann, K. *et al.* Generation of knock-in primary human T cells using Cas9 ribonucleoproteins. *Proc. Natl. Acad. Sci.* **112**, 10437–10442 (2015).

74. Adli, M. The CRISPR tool kit for genome editing and beyond. *Nat. Commun.* **9**, 1–13 (2018).

75. Marafioti, T. *et al.* Expression of B-Lymphocyte-Associated Transcription Factors in Human T-Cell Neoplasms. *Am. J. Pathol.* **162**, 861–871 (2003).

76. Kang, S. M. *et al.* Induction of the POU domain transcription factor Oct-2 during T-cell activation by cognate antigen. *Mol. Cell. Biol.* **12**, 3149–3154 (1992).

77. Smith, I. *et al.* Evaluation of RNAi and CRISPR technologies by large-scale gene expression profiling in the Connectivity Map. *PLOS Biol.* **15**, e2003213 (2017).